Sede Amministrativa: Università degli Studi di Padova

Dipartimento di Biologia

SCUOLA DI DOTTORATO DI RICERCA IN BIOSCIENZE E BIOTECNOLOGIE
INDIRIZZO: BIOLOGIA CELLULARE
CICLO XXVI

THE ROLE OF DEOXYNUCLEOTIDE TRAFFICKING AND DEGRADATION IN THE MAINTENANCE OF BALANCED POOLS OF DNA PRECURSORS IN MAMMALIAN CELLS

Direttore della Scuola : Ch.mo Prof. Giuseppe Zanotti
Coordinatore d'indirizzo: Ch.mo Prof. Paolo Bernardi
Supervisore : Ch.mo Prof. Vera Bianchi

Dottoranda : Cristina Miazzi

TABLE OF CONTENTS

LIST OF ABBREVIATIONS

A_{600}	Absorbance at 600 nm
ADA	Adenosine deaminase
ADP	Adenosine diphosphate
AdR	Deoxyadenosine
AMP	Adenosine monophosphate
ANC	Adenine nucleotide carrier
ATP	Adenosine triphosphate
BCA	Bicinchoninic acid
BrdU	Bromodeoxyuridine
BSA	Bovine serum albumin
CDK1	Cyclin-dependent kinase 1
cdN	Cytosolic 5'-deoxynucleotidase
cDNA	Complementary DNA
CDP	Cytidine diphosphate
CdR	Deoxycytidine
CMP	Cytidine monophosphate
CNT(s)	Concentrative nucleoside transporter(s)
Cpm	counts per minute
CTP	Cytidine triphosphate
d	Days
D. melanogaster	Drosophila melanogaster
dADP	Deoxyadenosine diphosphate
dAMP	Deoxyadenosine monophosphate
DAPI	4',6-diamidino-2-phenylindole
dATP	Deoxyadenosine triphosphate
dCDP	Deoxycytidine diphosphate
dCK	Deoxycytidine kinase
dCMP	Deoxycytidine monophosphate
dCTP	Deoxycytidine triphosphate
dGDP	Deoxyguanosine diphosphate
dGK	Deoxyguanosine kinase
dGMP	Deoxyguanosine monophosphate
dGTP	Deoxyguanosine triphosphate
DMEM	Dulbecco's modified Eagle's medium
dN(s)	Deoxynucleoside(s)
DNA	Deoxyribonucleic acid
DNC	Deoxynucleotide carrier
dNDP(s)	Deoxynucleoside diphosphate(s)
dNMP(s)	Deoxynucleoside monophosphate(s)
dNTP(s)	Deoxynucleoside triphosphate(s)
dTDP	Thymidine diphosphate

dTMP	Thymidine monophosphate
DTT	Dithiothreitol
dTTP	Thymidine triphosphate
dUDP	Deoxyuridine diphosphate
dUMP	Deoxyuridine monophosphate
dUTP	Deoxyuridine triphosphate
E. coli	Escherichia coli
E. faecalis	Enterococcus faecalis
ECL	Enhanced chemiluminescence
EDTA	Ethylenediaminetetraacetic acid
EGTA	Ethylene glycol-bis(2-aminoethylether)-*N,N,N',N'*-tetraacetic acid
ENT(s)	Equilibrative nucleoside transporter(s)
FCS	Fetal calf serum
GAPDH	Glyceraldehyde 3-phosphate dehydrogenase
GDP	Guanosine diphosphate
GdR	Deoxyguanosine
GTP	Guanosine triphosphate
HEK293	Human embryonic kidney 293 cells
HIV-1	Human immunodeficiency virus type 1
HOS	Human osteosarcoma cells
HPLC	High-performance liquid chromatography
IFN-γ	Interferon gamma
IPTG	Isopropyl β-D-1-thiogalactopyranoside
kDa	kilo Dalton
LB	Luria-Bertani broth
LINE-1	Long interspersed elements 1
mdN	Mitochondrial 5'-deoxynucleotidase
MDS(s)	Mitochondrial DNA depletion syndrome(s)
MNGIE	Mitochondrial neurogastrointestinal encephalopathy
MOPS	3-(N-morpholino) propanesulfonic acid
mRNA	Messanger RNA
mt	Mitochondrial
NDP(s)	Nucleoside diphosphate(s)
NDPK(s)	Nucleoside diphosphate kinase(s)
Ni-NTA	Nickel-nitrilotriacetic acid
OD	Optical density
Ost	Human osteosarcoma TK1⁻ cells

PBS	Phosphate Buffered Saline
PCA	Percloric acid
PCR	Polymerase chain reaction
PNC1	Pyrimidine nucleotide carrier 1
PNP	Purine nucleoside phosphorylase
PVDF	Polyvinylidene difluoride
RNA	Ribonucleic acid
RNR	Ribonucleotide reductase
SAMHD1	Sterile alpha motif and HD-domain containing protein 1
SDS-PAGE	Sodium Dodecyl Sulphate - PolyAcrylamide Gel Electrophoresis
shRNA(s)	Short hairpin RNA(s)
siRNA(s)	Small interfering RNA(s)
SLC25	Solute carrier family 25
T. termophilus	Thermus termophilus
T-PBS	PBS + 0.05% Tween 20
TdR	Thymidine
TK1	Thymidine kinase 1
TK2	Thymidine kinase 2
TMPK	Thymidylate kinase
TP	Thymidine phosphorylase
TYMS	Thymidylate synthase
UCP1	Uncoupling protein 1
UDP	Uridine diphosphate
UdR	Deoxyuridine
UMP	Uridine monophosphate
UQCRFS1	Ubiquinol cytochrome C reductase
UR	Uridine
UTP	Uridine triphosphate
WT	Wild type

SUMMARY

Deoxynucleoside triphosphates (dNTPs) are the precursors for DNA synthesis. Their balanced concentrations ensure the accuracy of nuclear and mitochondrial DNA replication and of DNA repair. dNTP pool sizes and relative proportions are regulated by a network of anabolic and catabolic enzymes, operating in the cytosol and in mitochondria. Cytosolic and mitochondrial pools are separated by the impermeable inner mitochondrial membrane but multiple evidences suggest the existence of mitochondrial carriers mediating the transport of deoxynucleotides between the two compartments. PNC1 has been identified as a pyrimidine nucleotide carrier by reconstitution in liposomes and its involvement in the import of UTP into mitochondria has been confirmed in human cells.

The main enzyme synthesizing dNTPs is the cytosolic ribonucleotide reductase (RNR). It provides the four DNA precursors in balanced amounts through a tight regulatory mechanism based on two distinct allosteric sites controlling catalytic activity and substrate specificity. Alternatively, dNTPs derive from the salvage of deoxynucleosides by subsequent phosphorylation steps in the cytosol and in mitochondria. Catabolic enzymes mediate the dephosphorylation of deoxynucleoside monophosphates and the degradation of deoxynucleosides. SAMHD1 is a recently identified catabolic enzyme with a dNTP triphosphohydrolase activity and is allosterically activated by dGTP to degrade the four dNTPs. It was first described as a restriction factor for HIV-1 infection in immune cells but its wide expression in most human tissues suggests that it may have a more general function.

The present work investigates the role of deoxynucleotide trafficking and degradation on the maintenance of dNTP pool balance focusing on three major issues: *(i)* the role of PNC1 in the trafficking of thymidine nucleotides in intact cells, *(ii)* the mechanism of allosteric regulation of SAMHD1 and *(iii)* its biological function in human cells.

We demonstrate that PNC1 is involved in the import of thymidine phosphates into mitochondria and in their export to the cytosol. Thymidine nucleotides are mostly synthesized *de novo* and by TK1-dependent salvage in the cytosol when cells are replicating their nuclear DNA, while the mitochondrial salvage of thymidine prevails outside S-phase. Thus, the bidirectional transport of thymidine nucleotides across the inner mitochondrial membrane maintains the intracellular equilibrium of the dTTP pool.

In human cells we find that SAMHD1 expression is cell-cycle regulated, highest in quiescence and minimal in S-phase. Manipulation of its expression through siRNAs disrupts the cell-cycle regulation of dNTP pools, which are present at low

levels outside S-phase and expand in S to support the replication of the nuclear genome. Disregulation of dNTP pools disturbs the normal progression of the cell cycle by interfering with the G1/S transition. We describe a key role for SAMHD1 and its catabolic activity in maintaining DNA precursors at low concentrations in the G1-phase to allow a correct transition into S. Through a biochemical characterization of the recombinant mouse and human proteins we demonstrate the existence of two distinct regulatory sites for the control of SAMHD1 activity. We suggest that a common regulatory mechanism based on allostery operates on the two opposed reactions catalyzed by RNR and SAMHD1 to set dNTP pool balance.

RIASSUNTO

Affinchè la sintesi del DNA possa avvenire con precisione, la cellula deve disporre di un pool bilanciato di precursori, i deossinucleosidi trifosfato (dNTP). Tale condizione non è limitata alla fase S, dove il genoma nucleare viene replicato, ma deve essere mantenuta per tutta la vita cellulare, al di fuori della fase S e in quiescenza, dove riparazione del DNA e replicazione del genoma mitocondriale hanno luogo. Lo stato di proliferazione cellulare determina la disponibilità di precursori del DNA: all'entrata in fase S il pool si espande per sostenere la replicazione del DNA nucleare; al termine, il pool si riduce notevolmente, mantenendosi a livelli sufficienti per garantire le altre attività di sintesi del DNA.

I quattro precursori (dATP, dCTP, dGTP e dTTP) costituiscono un pool bilanciato quando le concentrazioni intracellulari sono adeguate alle necessità cellulari e le rispettive proporzioni sono corrette. A questo scopo una rete di enzimi di sintesi e di degradazione regola finemente il metabolismo dei dNTP in due compartimenti subcellulari distinti, citosol e mitocondri, ognuno dei quali possiede un proprio corredo enzimatico.

La principale via di sintesi dei dNTP è rappresentata dalla riduzione di nucleosidi difosfato a deossinucleosidi difosfato nel citosol. Tale reazione è mediata dall'enzima ribonucleotide reduttasi (RNR), la cui attività è correlata allo stato di proliferazione cellulare e viene fortemente indotta all'ingresso in fase S. La RNR produce tutti i quattro dNTP ed è regolata da un meccanismo allosterico basato su due siti distinti che determinano, rispettivamente, l'attività catalitica e la specificità di substrato, assicurando un apporto bilanciato di precursori del DNA. La via di sintesi alternativa consiste nel recupero dei deossinucleosidi attraverso la loro fosforilazione nel citosol e nei mitocondri ed è mediata da chinasi specifiche di ciascun compartimento.

Le principali vie di degradazione sono catalizzate da 5'-nucleotidasi, citosoliche e mitocondriali, che convertono i deossinucleosidi monofosfato a deossinucleosidi e da fosforilasi che rimuovono i deossinucleosidi. A questi enzimi catabolici si è aggiunto recentemente SAMHD1, che nel nucleo converte i dNTP in deossinucleosidi, rimuovendo il gruppo trifosfato in un singolo passaggio. Attività enzimatiche simili erano già note in diversi procarioti e SAMHD1 ne è il primo esempio in cellule eucariotiche. SAMHD1 è in grado di defosforilare solo il dGTP se incubato con singoli deossinucleotidi, ma in presenza di dGTP la sua specificità di substrato diviene più ampia e può catalizzare anche la degradazione di dATP, dCTP e dTTP. Il dGTP, dunque, è sia substrato che effettore allosterico per l'enzima.

Alcune analogie con la RNR non sono sfuggite alla nostra attenzione: entrambi gli enzimi hanno la capacità di usare quattro diversi substrati e sono regolati in maniera allosterica da deossinucleosidi trifosfato. Questa osservazione ci ha spinto ad indagare in maggior dettaglio il meccanismo di regolazione di SAMHD1. A questo proposito, le proteine ricombinanti umana e murina sono state espresse in *E. coli* e purificate. La caratterizzazione biochimica è stata condotta in maniera approfondita con l'enzima murino; lo studio della proteina umana è attualmente in fase conclusiva. I risultati descritti sono stati ottenuti grazie ad un saggio enzimatico molto sensibile, basato sull'impiego di substrati marcati con radioisotopo, che ci ha consentito di misurare anche livelli minimi di attività. Abbiamo inizialmente identificato il GTP come un potente attivatore di SAMHD1, che induce l'enzima ad ampliare la sua specificità di substrato senza essere a sua volta degradato, diversamente dal dGTP. Il GTP, dunque, ci ha consentito di analizzare separatamente l'attività catalitica e la regolazione allosterica dell'enzima. SAMHD1 aveva apparentemente un'affinità molto bassa per il substrato dCTP, la cui degradazione non veniva affatto stimolata dal GTP nel range di concentrazioni 0-100 μM. Ci siamo chiesti se potessero esistere altri effettori allosterici capaci di regolare l'attività di SAMHD1 e, incubando l'enzima con diverse combinazioni di nucleotidi, abbiamo scoperto che dATP+GTP potenziano l'idrolisi dei deossinucleotidi pirimidinici (dCTP e dTTP). Il dATP, dunque, oltre ad essere substrato, funge anche da effettore allosterico per l'enzima, con il ruolo di attivatore secondario, perché esercita questa funzione solo in presenza di GTP, che assume quindi il ruolo di attivatore primario. Inoltre, GTP e dATP non competono per legarsi all'enzima e stimolarne l'attività. I risultati di questa caratterizzazione biochimica ci portano a concludere che esistano due siti distinti per la regolazione allosterica di SAMHD1. Dati cristallografici hanno recentemente confermato le nostre conclusioni e hanno dimostrato che i due siti allosterici hanno proprietà diverse: il primo è specifico per il (d)GTP, il secondo capace di ospitare il dATP ed eventualmente anche altri dNTP. Questo suggerisce che RNR e SAMHD1 siano regolati da un meccanismo allosterico molto simile, che opera sulle attività di sintesi e degradazione dei dNTP per garantire un pool bilanciato di precursori del DNA.

SAMHD1 è stato inizialmente identificato come il fattore di restrizione capace di contrastare la replicazione di HIV-1 in cellule del sistema immunitario mantenendo la concentrazione dei dNTP molto bassa. L'espressione di SAMHD1 si rileva in molti tessuti umani e in diverse linee cellulari, suggerendo un ruolo chiave per questo enzima che va al di là della funzione specializzata di protezione contro le infezioni lentivirali.

Per studiarne la rilevanza biologica, abbiamo scelto come modello sperimentale fibroblasti umani non trasformati. Mediante Western blot e immunofluorescenza abbiamo notato che SAMHD1 è soggetto a regolazione lungo il ciclo cellulare, con un livello di espressione minimo in fase S e massimo in quiescenza. Il silenziamento di SAMHD1 in colture proliferanti rallenta la crescita cellulare, bloccando le cellule in fase G1 e impedendone l'ingresso in S. Nonostante la ridotta percentuale di cellule in fase S, i pool dei quattro precursori del DNA sono presenti in concentrazioni elevate, con un aumento notevole del pool del dGTP rispetto a cellule di controllo non silenziate.

Manipolando l'espressione di SAMHD1 si interferisce con la sua regolazione lungo il ciclo cellulare; questo provoca un'espansione e uno sbilanciamento del pool in una fase in cui i dNTP sono solitamente presenti a basse concentrazioni. Tale condizione interferisce con la normale progressione del ciclo cellulare.

Quando gli siRNA vengono rimossi dal terreno di coltura, sono necessari 6-8 giorni affinchè la proteina torni ad essere espressa; durante questo periodo la dimensione dei pool rimane elevata e la crescita cellulare bloccata. Quando la proteina riappare, si ristabilisce una condizione di normalità, in termini di concentrazione di dNTP e proliferazione cellulare. Anche in cellule quiescenti il silenziamento di SAMHD1 provoca un espansione dei dNTP, con un aumento notevole del pool del dGTP, suggerendo che SAMHD1 contrasta un'attività di sintesi presente a livello basale anche in cellule post-mitotiche.

Questi risultati dimostrano che l'attività catabolica di SAMHD1 ha un ruolo chiave nel regolare la disponibilità di precursori del DNA nel corso del ciclo cellulare: in fase S i pool si possono espandere grazie alla stimolazione della loro sintesi e inibizione della loro degradazione; in fase G1 SAMHD1 mantiene i pool a concentrazioni ridotte, consentendo la normale progressione del ciclo cellulare.

Citosol e mitocondri possiedono un proprio corredo enzimatico per la regolazione dei precursori del DNA in ciascun compartimento. I pool citosolico e mitocondriale sono separati dalla membrana mitocondriale interna, che rappresenta una barriera impermeabile. Nonostante ciò, molte sono le evidenze sperimentali che sostengono l'esistenza di scambi di deossinucleotidi tra citosol e mitocondri, suggerendo l'esistenza di trasportatori mitocondriali dedicati. Nell'uomo, le proteine di trasporto mitocondriale sono codificate dai geni della famiglia *SLC25*. La proteina SLC25A33, omologa al trasportatore Rim2p in lievito, è stata rinominata PNC1 per la sua capacità di trasportare nucleotidi pirimidinici quando ricostituita in liposomi. In cellule umane è stato confermato il ruolo di PNC1 nell'importo di UTP all'interno dei mitocondri e nel mantenimento del genoma mitocondriale.

In questo lavoro abbiamo studiato in cellule umane il ruolo di PNC1 nel trasporto dei deossinucleotidi della timidina. L'approccio sperimentale che abbiamo adottato si basa su tre punti principali:

- I deossinucleotidi della timidina prodotti attraverso la via di recupero derivano dalla fosforilazione della timidina (TdR). Tale reazione è catalizzata dalla timidina chinasi (TK) 1 nel citosol e dalla TK2 nei mitocondri. Marcando le cellule per pochi minuti con ^{3}H-TdR, è possibile seguire il flusso intracellulare del precursore radioattivo. La variazione della radioattività specifica del precursore permette di valutare le dinamiche del pool e si è rivelata uno strumento molto utile per lo studio dell'attività di trasporto di PNC1.

- L'impiego di cellule proliferanti TK1$^+$ e TK1$^-$ ha permesso di studiare la direzione del trasporto. Infatti, in cellule TK1$^-$ la ^{3}H-TdR viene fosforilata dalla TK2 nei mitocondri e i deossinucleotidi marcati vengono poi esportati nel citosol; in cellule TK1$^+$ la ^{3}H-TdR viene fosforilata dalla chinasi citosolica, molto attiva in fase S, e i deossinucleotidi marcati vengono successivamente importati nei mitocondri.

- L'espressione di PNC1 è stata modulata attaraverso il silenziamento, stabile o transiente, e la sovraespressione inducibile.

In questo modo abbiamo stabilito che PNC1 media l'importo dei deossinucleotidi della timidina nei mitocondri e il loro esporto verso il citosol.

In cellule proliferanti la sintesi del dTTP avviene prevalentemente nel citosol, sede di un'attiva sintesi *de novo* e di recupero; in cellule quiescenti il contributo delle vie citosoliche si riduce notevolmente e aumenta l'attività di recupero mitocondriale. Il trasporto bidirezionale da parte di PNC1 garantisce l'equilibrio del pool del dTTP, citosolico e mitocondriale, nei diversi stati di proliferazione cellulare.

1. INTRODUCTION

DNA precursors (dATP, dCTP, dGTP, dTTP) are the substrates for DNA synthesis. Intracellular deoxynucleoside triphosphates (dNTPs) oscillate during the cell cycle: they are present at a low basal level outside S-phase, to sustain DNA repair and the replication of the mitochondrial genome, and peak in S-phase, to support the replication of nuclear DNA.

The fidelity of DNA synthesis requires a balanced supply of dNTPs, provided by a network of cytosolic and mitochondrial interrelated enzymes. The network regulates dNTP pools in response to changes in the environment and adjusts dNTP synthesis to the requirements of the cell, according to its proliferation state.

Genetic loss of synthesizing or degrading enzymes disturbs the regulation of DNA precursors, leading to pool imbalances and manifesting as severe diseases.

1.1   Overview of the enzymatic network for dNTP regulation

The enzyme network described in Fig. 1 coordinates synthesis and degradation of dNTPs in order to fine-tune the intracellular amount of DNA precursors [1].

The main source of dNTPs for DNA replication is *de novo* reduction of nucleoside diphosphates (NDPs) to deoxynucleoside diphosphates (dNDPs) in the cytosol. The key enzyme in this pathway is ribonucleotide reductase (RNR), which exists as R1/R2 isoform in S-phase and as R1/p53R2 isoform in proliferating and non-dividing cells. dATP, dCTP and dGTP are produced from reduction of ADP, CDP and GDP to the corresponding dNDPs, which are further phosphorylated by nucleoside diphosphate kinases (NDPKs) to dNTPs. *De novo* synthesis of dTTP requires additional steps: dUMP, deriving from the reduction of CDP and UDP in the cytosol, is converted to dTMP by thymidylate synthase (TYMS) in the nucleus [2] and in mitochondria [3]; dTMP is then phosphorylated to dTDP by thymidylate kinase (TMPK) and to dTTP by NDPKs.

Alternatively, new material can be introduced in the pool of dNTPs through salvage of catabolites. Deoxynucleosides (dN) coming from the degradation of cellular or exogenous DNA are exchanged across the plasma membrane. Concentrative sodium-dependent nucleoside carriers (CNT) actively transport (deoxy)nucleosides into the cells, while equilibrative nucleoside carriers (ENT) facilitate the diffusion of (deoxy)nucleosides [4]. The two families of nucleoside carriers include several members, differing in their substrate specificities and

tissue distributions. Among them, ENT1, which has a broad substrate specificity and is almost ubiquitously expressed, shuttles (deoxy)nucleosides across the plasma membrane and the inner mitochondrial (mt) membrane [5], thus integrating the intracellular metabolism of DNA precursors with the extracellular environment.

Deoxynucleosides enter the pool of DNA precursors through subsequent phosphorylation steps. The first is catalyzed by deoxynucleoside kinases, thymidine kinase 1 (TK1) and deoxycytidine kinase (dCK) in the cytosol or thymidine kinase 2 (TK2) and deoxyguanosine kinase (dGK) in mitochondria. The different substrate specificities of the kinases ensure the salvage of the four deoxynucleosides in both compartments: in the cytoplasm UdR and TdR are the substrates of TK1, while CdR, AdR and GdR are phosphorylated by dCK; in mitochondria TK2 is specific for TdR, UdR and CdR, while dGK phosphorylates GdR and AdR.
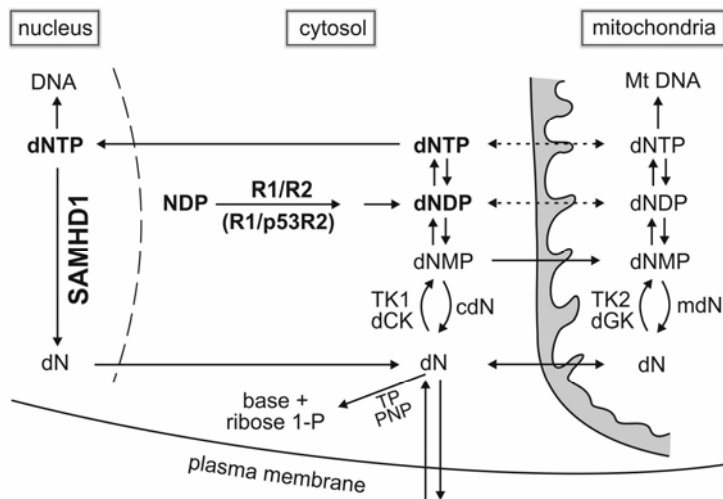

Fig. 1: Schematic representation of the enzymatic network for the regulation of dNTP metabolism.
dNTPs are synthesized through *de novo* ribonucleotide reduction in the cytosol (by the R1/R2 and R1/p53R2 isoforms of RNR) or salvage of deoxynucleosides (dN) in the cytosol (by TK1 and dCK) and in mitochondria (by TK2 and dGK). Deoxynucleotides are exchanged between the two compartments and their intracellular concentrations are regulated by catabolic activities: SAMHD1 degrades dNTPs to deoxynucleosides in the nucleus; 5'-deoxynucleotidases dephosphorylate dNMPs in the cytosol (cdN) and in mitochondria (mdN); deoxynucleosides can be either degraded by phosphorylases (TP and PNP) or exchanged across the plasma membrane and the inner mt membrane.

Catabolic enzymes remove material from the pool of dNTPs. SAMHD1 hydrolyses dNTPs to deoxynucleosides in the nucleus. 5'-nucleotidases dephosphorylate deoxynucleoside monophosphates (dNMPs) and convert them back to deoxynucleosides. Among the seven 5'-nucleotidases identified in man, the cytosolic (cdN) and the mitochondrial (mdN) 5'-deoxynucleotidases are

ubiquitously expressed and preferentially active on deoxyribonucleotides [6]. 5'-deoxynucleotidases and deoxynucleoside kinases form futile cycles (or substrate cycles) in cytosol and mitochondria. Deoxynucleosides can further be degraded by phosphorylases, i.e. thymidine phosphorylase (TP) and purine nucleoside phosphorylase (PNP), or deaminases in the cytosol.

Deoxynucleotide carriers are included in the network, although still incompletely defined. They exchange deoxynucleotides between cytosol and mitochondria, thus integrating the metabolism of DNA precursors in these subcellular compartments.

1.2 Cell-cycle dependent regulation of dNTP synthesis

The availability of DNA precursors in the cells is highly regulated during cell cycle and is strictly correlated with DNA replication [7].

In order to support the replication of the nuclear genome, cells increase their intracellular dNTP pools at least 10-fold as they are committed to enter S-phase. Pool expansion is generated by up-regulation of *de novo* synthesis and relies on induction of ribonucleotide reductase (R1/R2 isoform), whose activity is restricted to S-phase by means of transcriptional and post-translational control. Transcription of R1 and R2 genes is activated at the G1/S transition [8]. While R1 and R2 mRNAs increase in parallel and reach the same abundance in S-phase, the regulation at the protein level differs [9]. The R1 subunit is highly stable and constantly present throughout the cell cycle because of its long half-life. The R2 subunit has a fast turnover [10]. Its N-terminal KEN box targets the protein for complete degradation by the anaphase-promoting complex at the end of S-phase [11, 12]. Thus, R2 is the limiting factor for the formation of the S phase-specific R1/R2 complex.

De novo and salvage pathways for dTTP production are both cell-cycle regulated. *De novo* synthesis of dTTP is maximum in S-phase, when the complex for thymidylate synthesis becomes active through translocation to the nucleus [2] and dTMP can be phosphorylated by TMPK before the enzyme is degraded in mitosis [13]. Cytosolic salvage of TdR by TK1 is up-regulated when cells prepare to replicate their nuclear DNA. Although TK1 reaches a peak in protein level in mitosis, enzyme activity is restricted to S-phase by phosphorylation-dependent disruption of its tetrameric structure [14]. The C-terminal KEN box targets the protein for proteasomal degradation in late mitosis [15].

Outside S-phase and in resting cells, DNA precursors are present at a low basal level, yet sufficient to support DNA repair and mitochondrial DNA (mtDNA)

synthesis. They are provided by the salvage pathway and by *de novo* ribonucleotide reduction through the complex R1/p53R2.

p53R2 is homologous to the S phase-restricted R2 subunit and its expression is up-regulated in response to DNA damage through direct interaction with p53 [16]. It lacks a KEN box sequence for cell cycle regulation [11] and is constitutively expressed at a low level [17], with a 2-fold induction in quiescence [18]. The complex R1/p53R2 has a constant low activity, accounting for 2-3% of the S phase-specific RNR activity, and is essential for DNA repair and mtDNA synthesis outside S-phase [19].

In non-dividing cells the salvage of deoxynucleosides is mediated by the cytosolic dCK and the mitochondrial TK2 and dGK. TK2 activity increases 3-fold [20] and also dGK activity is slightly induced passing from the cycling to the quiescent state [21]; dCK is differentially regulated in human tissues, with the highest activity in leukocytes [22] and a slight downregulation in quiescent cells [21]. The stimulation of the mitochondrial salvage pathways at the expense of the cytosolic counterparts suggests that a cytosolic-mitochondrial communication is required to maintain the equilibrium in dNTP metabolism.

1.3   Interrelations between cytosolic and mitochondrial pools of deoxynucleotides

Several observations indicate that deoxynucleotides are exchanged between cytosol and mitochondria. Indeed, the mitochondrial toxicity of the antiviral nucleoside analogue 2'-3'-dideoxycytine depends on a phosphorylation event in the cytosol [23]. The crossing of the inner mitochondrial membrane can also be inferred from the flux of isotopic-labelled nucleosides in intact cells [21, 24]. Additional evidences of deoxynucleotide entry into mitochondria come from experiments with isolated organelles: a dCTP transport activity has been characterized and partially purified from mitochondria of leukemic cells [25] and a specific import of dTMP has been described in isolated mouse liver mitochondria [26]. Influx of deoxynucleotides into mitochondria is essential for the maintenance of the mitochondrial genome, as outlined by the consequences of p53R2 deficiency: the genetic inactivation of cytosolic *de novo* dNTP synthesis leads to depletion of mtDNA in differentiated cells [27].

Thus, the regulation of mtDNA precursors is among the metabolic processes that require the participation of intra- and extra-mitochondrial enzymes. The inner mitochondrial membrane is not permeable to deoxynucleotides, which require dedicate carriers to be transported between the two compartments. Despite

multiple evidences of their existence, the molecular nature of the mitochondrial deoxynucleotide carriers was not known for a long time.

In man, mitochondrial solute carriers are encoded by the *SLC25* gene family, whose members share conserved motives and a similar topology: they originate from three tandem-repeats of the same protein module, contain six trans-membrane α-helices and probably function as homodimers [28] (Fig. 2).
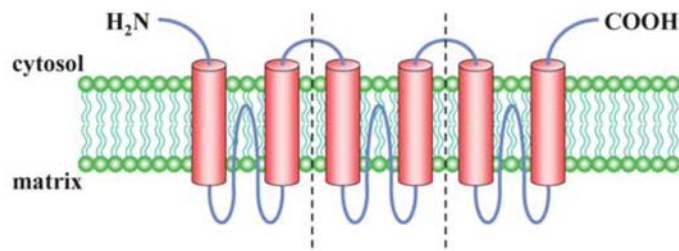

Fig. 2: Structural characteristics of the SLC25 family [28].
All mitochondrial carriers are characterized by three tandemly repeated homologous modules. Each module is about 100 amino acids in length and contains two hydrophobic α-helices, separated by hydrophilic regions and a loop protruding into the membrane. Both the N- and C- termini are located on the cytosolic side of the inner mt membrane.

A role in deoxynucleotide transport had been first assigned to SLC25A19, which shares putative motives for nucleotide binding with the mammalian peroxisomal adenine nucleotide carrier (ANC) and the uncoupling protein (UCP1). The recombinant protein reconstituted in liposomes was able to transport (deoxy)nucleotides and showed a higher affinity for dNDPs than for dNTPs. Hence, it has been renamed deoxynucleotide carrier (DNC) and has been proposed to exchange cytosolic dNDPs for mitochondrial ATP [29]. Further investigations and the characterization of a knock-out mouse revealed that SLC25A19 was instead a thiamine pyrophosphate carrier [30].

SLC25A33 and *SLC25A36* have recently been identified as members of the *SLC25* gene family [31]. The human proteins are related to the yeast mitochondrial nucleotide carrier Rim2p and to the homologous dRIM2 in the fruit fly.

Yeast Rim2p is selective for pyrimidine nucleotides [32], it exchanges thymidine, uridine and cytidine (deoxy)nucleotides and is essential for the maintenance of mtDNA [33]. In a recent study, the *D. melanogaster* dRIM2 is described to transport all four DNA precursors and to be essential for larval development and for the maintenance of mitochondrial functions (Caterina Da-Rè, Elisa Franzolin, Alberto Biscontin et *al*, Functional characterization of d*rim2*, the *Drosophila melanogaster* homolog of the yeast mitochondrial deoxynucleotide transporter, JBC, accepted on the 27th of January).

In man, the protein encoded by the gene *SLC25A33* is regulated by the insulin growth factor signalling pathway [34]. It was confirmed to exchange UTP and, to

a lesser extent, dTTP and CTP when reconstituted in liposomes and therefore was renamed pyrimidine nucleotide carrier (PNC1). Accordingly, silencing of PNC1 in cultured human cells causes a decrease in mitochondrial UTP content [34]. Downregulation of PNC1 has been reported to interfere also with cell proliferation and the replication of the mitochondrial genome [35].

Our work aims at further elucidating the transport activity of SLC25A33 (PNC1) and the related SLC25A36. We investigate their involvement in the trafficking of thymidine nucleotides in intact cells, where the carriers are exposed to physiological concentrations of nucleotides.

1.4   How cells establish and maintain balanced dNTP pools

The four DNA precursors are not only regulated in size, but also in their relative abundance: a balanced concentration of dNTPs is a pre-requisite for accurate DNA synthesis and is achieved through regulation of synthesis and degradation.

Allosteric regulation of ribonucleotide reductase

The same enzyme responsible for pool expansion in S-phase also ensures a balanced supply of dNTPs, through the coordinated synthesis of all four deoxynucleotides [36, 37].

Ribonucleotide reductase is a tetramer consisting of two copies of a large subunit (R1) and two of a small subunit (R2 or p53R2). Both subunits participate in the formation of the catalytic site (Fig. 3): R1 binds the substrates and contributes key residues for the redox reaction generating deoxyribonucleotides, the small subunit contributes the free tyrosyl radical which triggers the reaction.
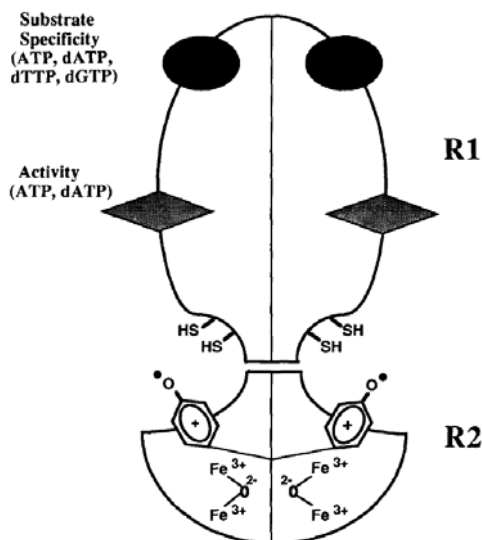

Fig.3: Schematic structure of RNR [38].
RNR is a heterotetramer. The R1 subunits contain the allosteric sites for the regulation of substrate specificity and catalytic activity. The R2 subunits generate the free tyrosyl radical, in a reaction involving a di-iron center and molecular oxygen. Catalysis requires the first radical provided by R2 and key residues provided by R1.

R1 harbours two allosteric sites for the regulation of enzyme activity and substrate specificity. The activity site senses the ATP/dATP ratio and determines the overall activity of the enzyme: ATP activates the reduction of the four NDPs to the corresponding dNDPs, which are then phosphorylated to dNTPs and incorporated into DNA. When the ATP/dATP ratio decreases because newly synthesized dATP builds up, then ATP is replaced by dATP and the enzyme is turned off.

The specificity site accommodates the end products of the reaction, i.e. dNTPs, and determines which substrate is to be reduced. The specificity and the catalytic sites are connected by a flexible loop; each allosteric dNTP is associated with a unique loop conformation and directs the binding of its partner NDP as a substrate in the catalytic site (Fig. 4).
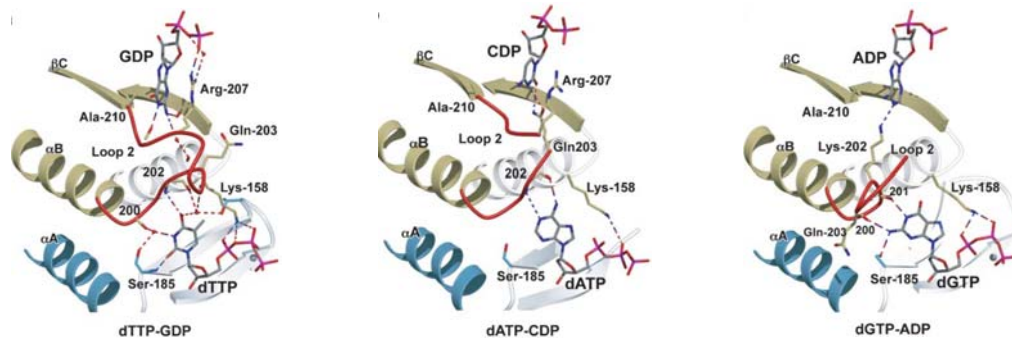

Fig. 4: Structural basis for the allosteric control of RNR substrate specificity [37].
Loop 2 (in red) is a flexible link between the allosteric specificity site and the catalytic site. Loop 2 rearrangements for each effector-substrate pair are shown.

Upon activation by ATP, deoxynucleotide synthesis begins with the reduction of CDP and UDP. dCTP is not an allosteric effector for the enzyme and dUDP is further converted to dTTP. When dTTP accumulates, it binds to the specificity site, shuts off the synthesis of pyrimidine deoxynucleotides and drives the reduction of GDP. When dGTP builds up, it replaces dTTP in the allosteric site, inhibits its own synthesis and shifts substrate specificity to ADP. Finally expansion of dATP pool completely turns off the enzyme (Fig. 5). Since ribonucleotide reduction is coupled with DNA replication, dNTPs are consumed through incorporation into DNA as they are synthesized. Consequently, accumulation of dATP and inhibition of enzyme activity may occur when DNA synthesis is complete.

Despite its sophisticated allosteric control, ribonucleotide reductase is not the only determinant of a balanced dNTP pool. The role of degrading enzymes will be described in the following sections.
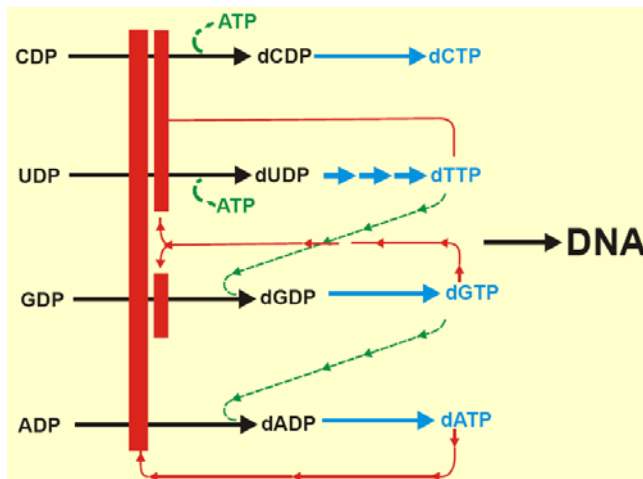
Fig. 5: Allosteric regulation of ribonucleotide reduction (modified from [36]).
Reduction of NDPs to the corresponding dNDPs is shown in black; further reactions producing dNTPs are indicated by blue arrows. Ribonucleotide reduction is allosterically activated by ATP, dTTP and dGTP (green arrows) and is allosterically inhibited by dTTP, dGTP and dATP (red arrows).

Substrate cycles

Cytosolic and mitochondrial substrate cycles are formed by the combination of irreversible opposing reactions [1, 7] (Fig. 6).

The anabolic arm is represented by deoxynucleoside kinases, which introduce new material in the pool of dNTPs through the phosphorylation of deoxynucleosides. Deoxynucleoside kinases are allosterically inhibited by dNTPs when the pool has reached the appropriate concentration. Thus, DNA precursors orchestrate both *de novo* and salvage synthesis pathways to set pool balance.

The catabolic arm is represented by 5'-deoxynucleotidases. They remove material from the pool of dNTPs by dephosphorylating dNMPs back to deoxynucleosides. Their activity largely depends on substrate concentration.

Substrate cycles are futile cycles because they consume ATP to continuously turn over the pool. When DNA synthesis is going on, dNTPs are consumed through incorporation into DNA. Under these conditions the anabolic arm of the substrate cycles prevails to refill the pool.
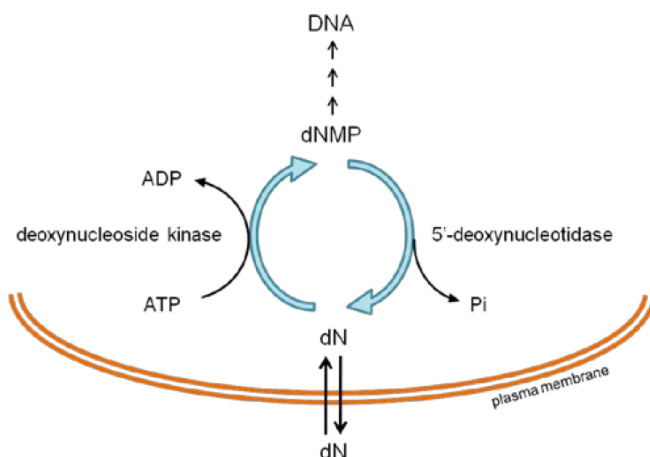

Fig. 6: Substrate cycle-mediated turnover in the pool.
In substrate cycles, deoxynucleosides (dN) are phosphorylated by deoxynucleoside kinases to dNMPs, which are then converted back to dN by 5'-deoxynucleotidases, with a net consumption of ATP.

20

The role of 5'-deoxynucleotidases becomes evident in the presence of a surplus of intracellular deoxynucleotides. Under these conditions the catabolic arm prevails and, together with phosphorylases, avoids a harmful expansion of dNTP pools.

SAMHD1

SAMHD1 has recently come into the network regulating dNTP metabolism. It was described in 2011 as a deoxynucleoside triphosphate triphosphohydrolase [39, 40]: it degrades dNTPs to deoxynucleosides by removing the triphosphate group in a single step. This unusual hydrolase activity had never been reported before in eukaryotes.

SAMHD1 is able to hydrolyze only dGTP when each dNTP is provided individually, but dATP, dCTP and dTTP can be efficiently hydrolyzed if dGTP is present as a cofactor. Catalytically active SAMHD1 is a tetramer [41, 42] with four catalytic sites and four allosteric sites. Each allosteric site binds dGTP and is formed by the contribution of three subunits. Thus, in addition to being the preferred substrate, dGTP is also the main regulator of enzyme activity: it drives oligomerization and interlocks the subunits in the tetramer. Tetramerization leads to reshaping of the substrate-binding pocket, which becomes catalytically active and able to accommodate all four dNTPs (Fig. 7).
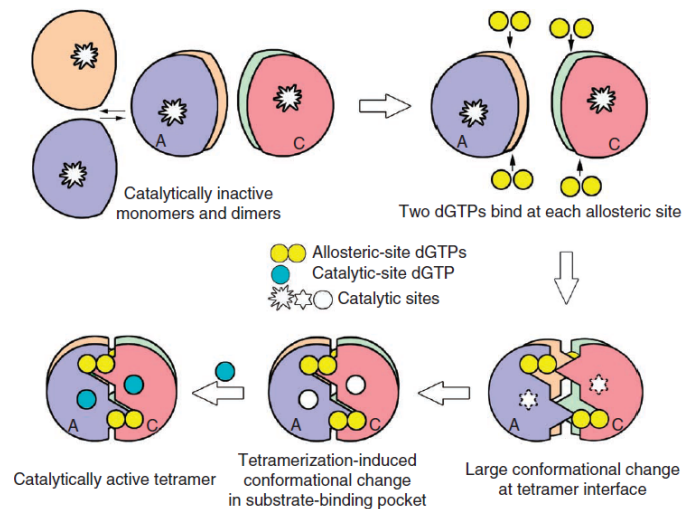

Fig. 7: dGTP-induced oligomerization and activation of SAMHD1 [42]**.**
Binding of four dGTP pairs at the allosteric sites induces large conformational changes, leads to tetramerization and reshaping of the substrate binding pocket, which becomes catalytically active.

Differently from all the other cytosolic and mitochondrial enzymes for dNTP regulation, SAMHD1 localizes in the nucleus [43]. The protein contains a N-terminal nuclear localization signal [44] followed by a SAM domain, a central catalytic HD domain and a C-terminal region for the stabilization of the tetramer. The SAM (sterile alpha motif) domain is among the most abundant interaction modules and mediates protein-protein and protein-nucleic acids interaction [45]. The HD domain is characterized by a conserved doublet of histidine (H) and aspartate (D) residues, as a signature of phosphohydrolase activity [46].

SAMHD1 was first identified in dendritic cells as a protein induced by interferon (IFN-γ) with a putative role in innate immunity [47]. It has been recently demonstrated to be the restriction factor responsible for early inhibition of HIV-1 replication in dendritic and myeloid cells [48]. Indeed, SAMHD1 is highly expressed in non-permissive cells and hampers the synthesis of viral DNA by depleting the intracellular pool of dNTPs [49].

In addition to its high expression in some cells of the immune system, SAMHD1 is present in most human tissues, including heart, skeletal muscles, spleen, liver and lung [47]. Enzymes showing a dNTP triphosphohydrolase activity have already been described in several prokaryotes: *E. coli* contains a dGTP-specific triphosphohydrolase [50]; a dNTP-dependent dNTPase from *T. termophilus* has a broad substrate specificity but requires dATP and dTTP as activating cofactors [51]; a dGTP-activated dNTP triphosphohydrolase has been characterized in *E. faecalis* [52].

So, dNTP triphosphohydrolases have an ancient origin and have been conserved by evolution up to humans. The widespread expression in several tissues and its maintenance during evolution suggested us that SAMHD1 could have a more general function beyond restriction of viral infections.

We also observed that SAMHD1 and RNR share some similarities: although they catalyze opposing reactions, they both are able to operate on four different substrates and use dNTPs to direct their substrate specificity. This led us to further elucidate the biochemical properties of SAMHD1 and its allosteric regulation.

1.5   Consequences of dNTP pool imbalance on genome stability

The complex enzymatic network described in Fig. 1 has the function to adjust synthesis and degradation rates depending on the intracellular requirements and the extracellular environment, in order to keep DNA precursors in balance. When cells are committed to replicate their nuclear DNA, dNTP pools become larger but are immediately used for DNA synthesis and the amount of each DNA precursor at any given moment in S-phase is only enough for the replication of a short fragment of the entire genome [7]. So, dNTP production is strictly coupled to DNA synthesis and balanced pools are of critical importance as they ensure the accuracy of the process. Indeed, even a mild pool imbalance may affect the fidelity of DNA synthesis, thus increasing the mutation rate and leading to genome instability [53].

Pool imbalance originates from a change in the relative proportions among DNA precursors, including expansion and/or depletion of one or more dNTPs. The most frequent mutations are misinsertions of a dNTP present in large excess. DNA polymerases are endowed with proofreading activities, which allow them to remove misplaced dNTPs. However, a misinsertion can be fixed depending on the context: when the dNTPs that have to be incorporated next to the misplaced one are present in excess, they favour polymerization at the expense of proofreading and a rapid extension occurs [54, 55]. In addition to misinsertions, pool imbalance may increase the frequency of insertions and deletions of nucleotides through misalignment of the template [55]. Single or double strand breaks may also appear because of inefficient DNA repair and may lead to gross chromosomal abnormalities [54]. Thus, a balanced level of dNTPs is essential for accurate base pairing, proper functioning of editing activities within DNA polymerases and efficacy of DNA repair.

Pool imbalance can be experimentally induced by addition of exogenous deoxynucleosides, chemical inhibition of enzymes, selection of mutant cells [54] or manipulation of RNR specificity [53].

In humans some genetic deficiencies perturb dNTP regulation, cause pool imbalance and lead to severe diseases. Early examples are adenosine deaminase (ADA) deficiency, where immune cell depletion is caused by a large increase in dATP pool [56], and PNP deficiency, where purine dNTP pool expansion and concomitant pyrimidine dNTP pool depletion [57] result in T-lymphocyte-specific toxicity [58].

Pool imbalance also interferes with the stability of the mitochondrial genome. Genetic inactivation of other four enzymes in the network causes severe mtDNA depletion syndromes (MDSs). MDSs are heterogeneous in phenotype but share a common decrease in mtDNA level in the most energy-demanding tissues,

including skeletal muscles, brain, heart, liver and kidney [59]. TP deficiency manifests as a mitochondrial neurogastrointestinal encephalopathy (MNGIE) [60], dGK deficiency is responsible for a hepatocerebral form of MDS [61] and muscles are mainly affected in TK2 and p53R2 deficiencies [27, 62]. Loss of synthesizing enzyme activities, such as TK2, dGK and p53R2, causes dNTP depletion, while downregulation of catabolic enzymes, such as TP, produces dNTP pool expansion. Both excess and depletion of a single dNTP may interfere with the replication of the mtDNA.

In post-mitotic cells DNA precursors for mtDNA replication are supplied by cooperation of salvage and R1/p53R2-dependent *de novo* synthesis. The tissue-specificity of the MDSs described above suggests that in some tissues intramitochondrial salvage of deoxynucleosides by TK2 or dGK may be the preferential pathway, in some other tissues cytosolic ribonucleotide reduction via R1/p53R2 and subsequent import of deoxynucleotides into mitochondria may prevail.

2.   AIM

This thesis investigates the role of deoxynucleotide trafficking and degradation on the maintenance of dNTP pool balance, considering three major issues:

1) Trafficking of deoxynucleotides between cytosol and mitochondria contributes to pool balance, especially in post-mitotic cells. The pyrimidine nucleotide carrier PNC1 is currently the first identified mitochondrial deoxynucleotide carrier. Its substrate specificity was earlier characterized in reconstituted liposomes and its involvement in the import of UTP into mitochondria has been confirmed in cultured human cells. Here we investigate in intact cells the role of PNC1 in the transport of thymidine nucleotides. The results of this work have been published in the following paper:

E. Franzolin, C. Miazzi, M. Frangini, E. Palumbo, C. Rampazzo, V. Bianchi, The pyrimidine nucleotide carrier PNC1 and mitochondrial trafficking of thymidine phosphates in cultured human cells, Exp. Cell Res. 318 (2012) 2226-2236.

2) dNTP pool balance requires coordinated synthesis and degradation of the four DNA precursors. For this purpose the anabolic enzyme RNR undergoes a tight allosteric regulation of substrate specificity and catalytic activity. We ask if a similarly exquisite allosteric regulation may operate in parallel on the catabolic enzyme SAMHD1, a recently characterized dNTP triphosphohydrolase which displays an allosterically-induced broad substrate specificity. The experiments on this issue are been completed.

3) SAMHD1 is expressed in most human organs and has a deep evolutionary origin, which suggest a more general function for the enzyme than restriction of viral infections. Here we ask what is the relevance of its catabolic activity in the well-characterized enzymatic network for dNTP pool regulation in mammalian cells. The results of this work have been published in the following paper:

E. Franzolin, G. Pontarin, C. Rampazzo, C. Miazzi, P. Ferraro, E. Palumbo, P. Reichard, V. Bianchi, The deoxynucleotide triphosphohydrolase SAMHD1 is a major regulator of DNA precursor pools in mammalian cells, Proc. Natl. Acad. Sci. U. S. A. 110 (2013) 14272-14277.

3.   EXPERIMENTAL PROCEDURES

3.1   Study of PNC1 transport activity in intact cells

Materials - [5-methyl-^{3}H]Thymidine (20,000 cpm/pmol) and [5-^{3}H]Uridine (25,000 cpm/pmol) were from PerkinElmer. The primary antibodies used were anti-human SLC25A33 rabbit polyclonal antibody (GTX106785, GeneTex) and anti-human ubiquitol cytochrome C reductase (UQCRFS1) (a subunit of complex III of the mt respiratory chain) mouse monoclonal antibody (ab 14746) from Abcam. Secondary antibodies were ECL-peroxidase labelled anti-rabbit NA934VS and anti-mouse NA931VS polyclonals from GE-Healthcare.

Cell lines and cell growth - The human tumor cell lines Ost TK1$^-$ and HOS TK1$^+$ were routinely grown in DMEM (Gibco) plus 10% heat-inactivated FCS (Gibco) and antibiotics [24]. Ponasterone-inducible Ost TK1$^-$ 20.7 [63] and HEK293-2-100 [64] cells, isolated previously in our laboratory, were transfected with an inducible expression vector carrying the PNC1 coding sequence to obtain stable clones with inducible overexpression of PNC1 (see below). All cell lines were periodically tested for Mycoplasma contamination by a PCR-based procedure (Minerva Biolabs). In each experiment the percentage of S-phase cells was checked by flow cytometry after propidium iodide staining with a BD-FACSCanto II Flow cytometer (BD Biosciences) and Moltfit software.

Transfection protocols for silencing of PNC1 and SLC25A36 - We transfected Ost TK1$^-$ cells with pRS retroviral silencing plasmids (OriGene) coding for shRNAs targeting the mRNA for PNC1. Downregulation was evaluated by measuring the residual mRNA levels by reverse-transcription real-time PCR. Stable clones were isolated in the presence of 0.5 µg/ml puromycin and 50 µg/ml uridine to prevent interference with pyrimidine *de novo* synthesis due to mitochondrial dysfunction [65]. Clones with >80% PNC1 downregulation were obtained only after transfection with pRS # TI329483. Controls were clones transfected with the empty vector. To silence PNC1 by additional interfering RNAs we used transient siRNA transfections with Stealth siRNA SLC25A33 HSS149886, SLC25A33 HSS 149887 and SLC25A33 HSS 149888 (Invitrogen). As controls we used two nontargeting siRNAs with GC compositions comparable to those of the targeting sequences. In the case of SLC25A36 we achieved a >90% downregulation by transfection with a cocktail of four different siRNAs (ON-TARGET plus SMART Pool l-007327-01-0010, Dharmacon). Parallel cultures were transfected with a pool of non-targeting siRNAs (D-001810-10-20). The transfections with siRNAs were performed according to the suppliers' instructions with the respective

liposomal preparations, RNAiMAX lipofectamine (Invitrogen) and Dharmafect 1 (Dharmacon) in medium without antibiotics. Transfections with Stealth siRNAs could not be prolonged beyond 48 h without eliciting signs of toxicity. Therefore cells were plated in 10-cm Petri dishes at 0.35 million Ost TK1$^-$ cells/plate and 24 h later the siRNA/liposome mix was added at 1 nM final concentration. Labelling experiments were performed after 48 h of transfection. Transfections with Dharmacon siRNAs did not cause any apparent toxicity. The cells were seeded at 2 x 10^6 cells/10 cm plate and after 24 h were transfected with 70 nM Smart Pool siRNAs. The following day the cultures were trypsinized, reseeded at 0.5 x 10^6 cells/10 cm plate in the presence of 35 nM siRNAs and maintained for 96 h before performing the isotope experiments.

Inducible overexpression of PNC1 - We subcloned into plasmid pIND (Invitrogen) the PNC1 cDNA obtained by PCR from I.M.A.G.E. full length cDNA clone IRAT p970D05105D (ImaGenes) using forward primer 5'-CATAAAGCTTGCCATGGCGAC GGCGGCCA-3' that introduced a *Hind*III site and reverse primer 5'-CTGAGGATCC TTACTGAGTACGGTCTTCTA-3', that introduced a *Bam*HI site. Plasmid pIND-PNC1 was transfected for 24 h into 90% confluent cultures of HEK293-2-100 [64] or Ost TK1$^-$ 20.7 [63] cells adding 7 μg DNA plus Lipofectamine 2000 (Invitrogen) per 5-cm plate in 5 ml growth medium without antibiotics. The following day the transfection medium was replaced with normal growth medium plus antibiotics. After 24 h 100 μg/ml zeocin and 800 μg/ml G418 were added and selection continued for one week. The transfected cells were then subcultivated in clonal culture and kept under continuous selection for two more weeks. The isolated clones were screened on the basis of their responsiveness to 48 h induction with 4 μM ponasterone (Sigma). Overexpression of PNC1 was evaluated by measuring the mRNA level by reverse-transcription real-time PCR and confirmed by immunoblotting.

RNA extraction, reverse transcription and real-time PCR - We extracted total RNA from 2 x 10^6 cells with TRIzol reagent (Invitrogen) and prepared cDNAs by reverse transcription with random hexamer primers and RNAse inhibitor (both from Applied Biosystems) and SuperScript II Reverse Transcriptase (Invitrogen). Real time PCR was performed with forward primer 5'-ATGGCATTTTCGTGCCT44C-3' and reverse primer 5'-TCTAGCTGCATTCGGGTTTT-3' and Power SYBR Green PCR master mix (Applied Biosystems) as described earlier [66]. To standardize target gene expression we chose as reference hydroxymethylbilane synthase that was expressed at levels comparable to those of PNC1 in control cells. In each run, each cDNA preparation was analyzed in triplicate. We employed the comparative Ct method [67] for data processing.

Immunoblotting - Protein extracts were prepared from 25 million HEK293 cells or 15 million Ost cells, induced to overproduce PNC1 by incubation with 1 or 4 μM ponasterone for 48 or 72 h. The plates were washed three times with ice-cold PBS and scraped with a rubber policeman in 500 μl extraction buffer (70 mM sucrose, 220 mM mannitol, 5 mM MOPS-Tris pH 7.4, 2 mM EGTA-Tris, 0.2 mg/ml BSA) plus 100 μM digitonin. The cell suspensions were lysed by aspiration in a syringe through a 23G x 1 ¼-inch needle, 5 strokes, followed by addition of 500 μl digitonin-free extraction buffer. Nuclei were pelleted by 5 min centrifugation at 1300 x g at 4°C. After transferring the supernatant to a new tube, we separated the mitochondria by centrifugation at 19,000 x g at 4°C, 20 min. The mitochondrial pellet was resuspended in 100 μl PBS containing 1.5% SDS and mammalian protease inhibitors (Sigma), incubated 30 min on ice and centrifuged for 10 min at 19,000 x g at 4°C. The protein concentration of the supernatant was determined by the BCA protein assay (Pierce). For electrophoresis on 4-15% polyacrylamide gels we loaded 10 μg HEK293 proteins per lane or 20 μg Ost proteins. After electrophoretic separation, the blots were processed as described [18, 66], using the anti-human SLC25A33 rabbit polyclonal antibody at 1:1000 dilution and the anti-human ubiquitol cytochrome C reductase (UQCRFS1) monoclonal at 1:8000 dilution. After incubation with the appropriate horseradish peroxidase-conjugated antibodies and washing, we detected and quantified the stained bands by a ECL-advanced kit (GE-Healthcare) and ImageJ software.

Isotope experiments - Labelling experiments were run 48 h from seeding in the case of stable clones of Ost TK1^{-} cells with PNC1 silencing or after 72 h induction with ponasterone in the case of overexpressing clones of Ost TK1^{-} or HEK293 cells. With Ost TK1^{-} cells transiently transfected with anti-PNC1 siRNAs labelling took place after 48 h of transfection. Cells with transient SLC25A36 silencing were pulse-labelled after a total of 5 days in the presence of siRNAs.

Before addition of isotope we substituted the medium with fresh pre-warmed medium with dialyzed serum and left the cultures to equilibrate for 2 h. All manipulations took place in a 37°C room to avoid thermal shocks. TK1-deficient cells were incubated with 1 μM ^{3}H-TdR for 5-40 min. TK1-proficient cells were instead incubated with 0.3 μM ^{3}H-TdR. Tritiated uridine was added at 0.1 μM concentration for 2-10 min. At the end of the isotope incubations the plates were moved to a cold room in a melting ice bath. Cells were washed with ice-cold PBS, scraped from the plates and homogenized by repeated aspiration through needles of different size: 23G 1 ¼ in. for Ost TK1^{-} cells, 21G for HOS TK1^{+} cells and 22G 1 ¼ in. for HEK293 cells. The mt and cytosolic nucleotides were separated by diffetential centrifugation of cell homogenates and nucleotide pools were extracted with ice-cold methanol as described [24]. The

mitochondrial/nuclear pellet remaining after methanol extraction was dissolved in 1 ml 0.3 M NaOH and used for nuclear DNA analysis. We precipitated portions of the alkali lysate with 0.3 M HClO$_4$, filtered the precipitate onto glass fiber filters and determined its radioactivity by liquid scintillation counting in a PerkinElmer Tricarb 2800 counter.

Pool determinations - The size and specific radioactivity of dTTP pools was measured by the DNA polymerase-based assay according to Sherman and Fyfe [68] with the modifications introduced by Ferraro et al [69]. The phosphorylation of ^{3}H-uridine to uridine phosphates was determined by a filter binding assay with Whatman DE-81 disks by spotting aliquots of pool extracts on the filters, washing three times with 5 mM NH$_4$-formate and eluting with 0.1 M HCl 0.2 M NaCl. Radioactivity retained by the filter represented the sum of UMP, UDP and UTP. During a 10-min pulse, corresponding to the longest incubation time, no detectable conversion of UDP to deoxynucleotides took place. To check for conversion of uridine to cytidine nucleotides, 30 µl of cytosolic extract from cells labelled with 0.1 µM ^{3}H-uridine were added to 70 µl H$_2$O and 100 µl 2 M PCA. The mix was boiled for 10 min and neutralized with 4 M KOH. After 10 min precipitation on ice the sample was centrifuged at 19,000 x g for 10 min at 4°C. The clear supernatant was loaded onto a Dowex 50 200-400 mesh column together with 1 µmole UMP and CMP carriers and eluted with 0.2 M acetic acid at a flux of 0.2 ml/min. Fractions of 2 ml were collected and analyzed for OD at 260, 280 and 310 nm and for radioactivity by scintillation counting.
The concentrations of the four ribonucleoside triphosphates and ADP in mt and cytosolic pools were measured by HPLC on a Partisil 10 SAX column (Whatman) with 0.4 M NH$_4$H$_2$PO$_4$ pH 5 as the mobile phase. Elution times were ADP 6 min, UTP 10 min, CTP 14.5 min, ATP 16.5 min and GTP 31 min.

Isolation of mitochondria from cultured cells, transport assays and pool determination - HEK293 clones were seeded in 15-cm dishes at 4 x 10^6 cells/plate and after 48 h ponasterone was added at 4 µM final concentration to induce the overexpression of PNC1. After 72 h, cells were washed with ice-cold PBS, scraped in buffer A (70 mM sucrose, 220 mM mannitol, 5 mM MOPS-Tris buffer pH 7.4, 2 mM EGTA-Tris, 0.2 mg/ml BSA) and homogenized by aspiration through a 26G needle, 6 strokes. Nuclei were pelleted by 10 min centrifugation at 900 x g at 4°C. The supernatant was transferred to a new tube and mitochondria were separated by centrifugation at 7,000 x g at 4°C, 10 min. The mitochondrial pellet was washed in buffer A and resuspended in 500 µl of 1M sucrose, 5 mM EDTA, 10 mM Tris-HCl pH 7.4. Mitochondria were loaded on a sucrose gradient, with a lower phase of 1.5 M sucrose, 5 mM EDTA, 10 mM Tris-HCl pH7.4 (3 ml) and a upper phase of 1 M sucrose, 5 mM EDTA, 10 mM Tris-HCl pH7.4 (3 ml), and

centrifuged for 40 min at 40,000 x g at 4°C. After centrifugation, purified mitochondria were collected, buffer A was added and the suspension was centrifuged for 10 min at 7,000 x g at 4°C. The mitochondrial pellet was resuspended in 70 µl of 250 mM sucrose, 10 mM Tris-HCL pH 7.4, 0.1 mM EGTA-Tris pH 7.4. The transport experiments were started by adding the mitochondrial suspension to buffer B (220 mM mannitol, 70 mM sucrose, 5 mM MOPS-Tris buffer pH 7.4, 0.1 mM EGTA-Tris, 1 mM phosphate-Tris pH 7.4, 1 mM $MgCl_2$, 5 mM glutamate, 2.5 mM malate, 0.2 mg/ml BSA) containing ^{3}H-substrates in a final volume of 0.3 ml. The incubations were performed on a shaker at 25°C. After the indicated time we cooled the incubation mixtures in glass vessels in an ice bath for 3 min and centrifuged them for 10 min at 19,000 x g at 4°C. We removed the supernatant and washed the sediment twice with 1 ml of buffer B without suspension. We extracted the sediment with ice-cold methanol, as described [24]. We determined the ATP/ADP/AMP, dTTP/dTDP/dTMP and dUTP/dUDP/dUMP ratios by HPLC on a C-18 column (Phenomenex) by isocratic elution (1-18 min at 0.5 ml/min, then 1 ml/min) with 0.2 M $NH_4H_2PO_4$ pH 3.5 for 35 min, followed by a 20 min gradient to 30% methanol. Nucleotides were quantified from the area on the chromatogram or, in transport experiments, by radioactivity. All values were normalized to 1 mg of mitochondria.

3.2 Expression, purification and characterization of recombinant SAMHD1

Materials - [8-^{3}H(N)]-dATP, [5,5-^{3}H]-dCTP, [8-^{3}H(N)]-dGTP and [methyl-^{3}H]-dTTP were from Perkin Elmer; non-labelled nucleotides were from Sigma.

Expression of recombinant SAMHD1 - The plasmid for bacterial expression of mouse SAMHD1 has been kindly provided by Dr. F. Perrino [39]. The cDNA encoding residues 32-658 of mouse SAMHD1 is cloned in the pCDFDuet1 expression vector with a His$_6$-tag at the N-terminus. The resulting protein contains both SAM and HD domains. Mouse SAMHD1 was expressed in *E. coli* Rosetta (DE3) cells (Novagen). Bacteria were grown to a A_{600} = 0.5 at 37°C in LB medium, 200 rpm, then quickly cooled on ice to 17°C and induced with 1 mM IPTG for 24h at 17°C, 180 rpm.

We received the plasmid for bacterial expression of human SAMHD1 from Dr. A. Yakunin [70]. The cDNA encoding full length human SAMHD1 (residues 1-626) is cloned in a modified pET15 expression vector with a N-terminal His$_6$-tag. The construct was transformed into *E. coli* BL21 (DE3) cells. Bacteria were grown to a A_{600} = 1 at 37°C in LB medium, 200 rpm, cooled to 16°C and induced overnight with 0.4 mM IPTG at 16°C, 180 rpm.

Purification of recombinant SAMHD1 - After induction with IPTG, a 500-ml culture was centrifuged and the bacterial pellet (2.9 g) was frozen at -80°C. It was then suspended in 6 ml of 50 mM Tris-HCl pH 7.5, 0.5% Triton-X, 5 mM β-mercaptoethanol, 2 mM $MgCl_2$, 1 mM EDTA containing 0.5 mM NaCl, 25% glycerol, additioned with a cocktail of bacterial protease inhibitors (Sigma). Cells were lysed by incubation for 30 min at room temperature with 1mg/ml lysozyme. Streptomycin sulphate at the final concentration of 1% (w/v) was added to precipitate DNA and the suspension was centrifuged at 100,000 x g for 30 min at 4°C. The supernatant was centrifuged again at 100,000 x g for 2 h, 4°C. The recombinant proteins were purified by Ni-NTA affinity chromatography at 4°C. The clear supernatant was applied directly to a column of 1 ml Ni-NTA resin (Qiagen). Mouse and human recombinant SAMHD1 were allowed to bind to the resin under stringent conditions, i.e. in the presence of 20 mM imidazole, and washed in 0.1 M NaCl, 0.1% Triton-X, 5 mM β-mercaptoethanol, 25% glycerol, 20 mM imidazole. The recombinant proteins were obtained by stepwise elution with increasing concentration of imidazole, in the same buffer described above. The following concentrations of imidazole were used for the elution of mouse SAMHD1: 35-50-75-100-250-500 mM; for the elution of human SAMHD1 instead: 50-100-250 mM. Separate fractions were collected and assayed for protein concentration and SAMHD1 activity. Protein concentrations was determined by the method of Bradford with BSA as standard.

Mouse SAMHD1 was enriched in the 100-mM imidazole fraction, where a peak of proteins with dGTP-induced dATP triphosphohydrolase activity was recovered. Human SAMHD1 was enriched in the 250-mM imidazole fraction. These two fractions were stored in aliquots and were used for our experiments. Their purity was checked by gel electrophoresis (see below).

Enzyme assay - The nucleotide phosphohydrolase reactions contained 20 mM Tris-HCl pH 7.5, 5 mM $MgCl_2$, 2 mM DTT, 1 μM EDTA, 50 mM NaCl, 2.5 mM β-mercaptoethanol, 1 mg/ml BSA, 12.5% glycerol, the indicated nucleotides and the SAMHD1 enzyme. We used ^{3}H-labelled dNTPs (1,000-20,000 cpm/nmol) as substrates, while the allosteric effectors (GTP, dGTP, dATP) were not labelled; the concentrations are indicated in the text in the "Results and discussion" section. We used 30 ng (8 nM) or 50 ng (13 nM) mouse and 150 ng (40 nM) human recombinant SAMHD1, in order not to exceed 20% of substrate consumption in all kinetic experiments. The reactions were incubated for 20 min at 37°C in a final volume of 50 μl and stopped by addition of 1 ml 5 mM EDTA. The solution was passed through a 1-ml column of AG1-X2 resin to retain unreacted nucleotides. The deoxynucleosides produced during the reaction were

eluted with 4.5 ml of 50 mM acetic acid. The total radioactivity of the eluent was a measure of the rate of dNTP dephosphorylation (nmol ^{3}H-dN/min/mg).

Purity control of enzyme preparations - We checked the result of the purification procedure by SDS-PAGE and we excluded the presence of contaminating phosphatases by HPLC analysis of the products of the enzymatic reaction.

Mouse and human purified SAMHD1 (4 µg) were loaded on Mini-Protean TGX precast gels (Bio-rad), electrophoresed and stained for 40 min with 0.25% Coomassie Brilliant blue R-250 in 45% methanol 9% acetic acid. The gel was then washed in 10% methanol 7% acetic acid and showed a strong band at 75 kDa, as expected from the monomer molecular mass of SAMHD1.

^{3}H-dATP (100 µM 30,000 cpm/nmol) was incubated with 100 ng (27 nM) mouse or 300 ng (80 nM) human SAMHD1, under the assay conditions described above. After 20 min, the solution was injected into a nucleosil C18 column (Phenomenex) for HPLC analysis and chromatographed at 1 ml/min isocratically for 30 min with 0.2 M $NH_4H_2PO_4$ pH 3.5, followed by a 20 min gradient to 30% methanol. We collected 0.5 ml fractions and determined the total radioactivity in each fraction by liquid scintillation counting.

Analysis of kinetic data - The kinetic data were fitted with either Michaelis-Menten or allosteric sigmoidal equations using the Prism software (version 5.00, GraphPad Software, La Jolla, CA).

3.3 Study of SAMHD1 function in mammalian cells

Materials - We used two different siRNAs to target the mRNA of human SAMHD1 (NM_015474): FlexiTube siRNA Hs_SAMHD1_7 (Qiagen Cat. No. SI04243673) and siSAMHD1-3 siRNA reported in [48]. The AllStars Negative Control siRNA (Qiagen) was used as a negative control. The following antibodies were used: anti-human SAMHD1 mouse monoclonal clone [1A1] (ab128107; Abcam), anti-human R2 goat polyclonal (sc-10844; Santa Cruz Biotechnologies), anti-human R1 mouse monoclonal clone AD203 (MAB3033; Millipore) and anti-human glyceraldehyde-3-phosphate-dehydrogenase (GAPDH) mouse monoclonal (MAB374; Chemicon international).

Transfections with siRNAs - In proliferating cells we analyzed the effects of SAMHD1 silencing by seeding 0.2 x 10^6 skin or lung fibroblasts in 10-cm dishes in DMEM with 10% (vol/vol) FCS and transfecting them after 24 h with 5 or 1 nM siRNA, respectively. In preliminary experiments, the two siRNAs mentioned above gave similar results both in terms of SAMHD1 down-regulation and

inhibition of cell proliferation, as exemplified by results in Fig. 4 under section 4.3. We used siRNA Hs_SAMHD1_7 for most other experiments. To obtain quiescent skin and lung fibroblasts, we seeded 0.4 x 10^6 cells per 10-cm dish in DMEM plus 10% (vol/vol) FCS and cultured them for 7 d until confluence. We then transfected the confluent cells with siRNAs (final concentration 5 nM for skin fibroblasts and 2 nM for lung fibroblasts) in DMEM with dialyzed 0.1% FCS without antibiotics using RNAiMAX (Life Technologies) according to the manufacturer's instructions. Three days later the medium was diluted 1:1 with fresh medium + 0.1% FCS and the cells were kept for an additional 4 d in the presence of 2.5 nM or 1 nM siRNAs for skin and lung fibroblasts, respectively. The same cultures underwent a second transfection with 5 nM (skin fibroblasts) or 1 nM siRNAs (lung fibroblasts) in DMEM with 0.1% FCS and the samples were analyzed 3 d later. By this protocol the cells remained in the presence of the siRNAs for a total of 10 d without replating.

RNA extraction, reverse-transcription and real-time PCR - We quantified by reverse-transcription real-time PCR the mRNA of SAMHD1 with the Applied Biosystems 7500 Real Time PCR System (Apllied Biosystems). We extracted total RNA from 0.5 x 10^6 cells with TRIzol reagent (Invitrogen) and prepared cDNAs by reverse transcription. We performed real-time PCR assays in 96-well optical plates as described in [66] using Quantitect Primer Assay kits (Qiagen) with specific primers for SAMHD1 and ribosomal protein large P0 (RPLP0) taken as endogenous control for normalizations.

Western blotting - Pellets of 1-2 million cells were collected, washed with PBS and lysed with radioimmunoprecipitation assay (RIPA) buffer (10 mM Tris-HCl pH 7.4, 100 mM NaCl, 1% sodium deoxycolate, 0.1% SDS, 1% Nonidet P-40) containing a mixture of protease inhibitors for mammalian cells (Sigma). The extact was centrifuged at 19,000 x g for 20 min, the protein concentrations of the supernatant solutions were determined by the BCA protein assay (Pierce), and appropriate amounts of the solution were loaded on precast gels (Bio-Rad) and electrophoresed. The proteins were blotted on Hybond-C extra (GE Healthcare) in the case of ribonucleotide reductase subunits, R2 and p53R2, and GAPDH, and on PVDF for SAMHD1 (Millipore). Both membranes were saturated with 2% ECL Blocking Agent (GE Healthcare) for 1 h at room temperature and incubated overnight at 4°C with the primary antibody (anti-SAMHD1 dilution 1:4,000, anti-R2 dilution 1:2,000, anti p53R2 dilution 1:2,000 and anti-GAPDH 1:5,000). After three washings with PBS + 0.05% Tween 20 (T-PBS) for 10 min, the membranes were incubated with the appropriate horseradish peroxidase-conjugated secondary antibody (dilution 1:80,000) for 1 h at room temperature. After further washing the membranes were developed using a chemiluminescence ECL

kit (LiteAblotTurbo, Euroclone). The signals were detected on Kodak films and quantified with ImageJ software.

BrdU incorporation - We grew 3.5 x 10^4 lung fibroblasts on glass coverslips in 3.5-cm dishes and transfected them after 24 h with negative control or anti-SAMHD1 siRNA. At different time points after transfection the cells were incubated with 30 µM BrdU for 30 min at 37°C and fixed with 50 mM glycine, pH 2 + 70% ethanol for 20 min at -20°C. We scored BrdU incorporation by immunofluorescence using the Roche Applied Science labelling and detection kit. Nuclei were counterstained with 0.2 µg/ml DAPI.

Immunofluorescence - Cells were grown in 35-mm-thin-bottomed Petri dishes for high-end microscopy (Ibidi), fixed with 4% paraformaldehyde for 15 min at 37°C, permeabilized with 0.2% Triton-X for 10 min at 37°C and blocked with MAXblock blocking medium (Active-Motif) for 1 h at 37°C. The fixed cells were incubated with the indicated primary antibody for 1 h at 37°C (anti-SAMHD1 dilution 1:200, anti-R2 dilution 1:200, anti-R1 dilution 1:100). After three 10-min washes with T-PBS, the cells were incubated with the appropriate secondary antibody (dilution 1:500) for 1 h at 37°C. After washing with T-PBS the cells were counterstained with 0.2 µg/ml of DAPI in a mounting medium for fluorescence microscopy. The immunostained cells were visualized using a Leica TCS SP5 confocal microscope equipped with 63X oil immersion objective.

Analytical procedures - Intracellular concentration of the four dNTPs were determined by an enzymatic assay [68] modified as described recently [69].

4.   RESULTS AND DISCUSSION

4.1   The pyrimidine nucleotide carrier PNC1 and mitochondrial trafficking of thymidine phosphates in cultured human cells.

In our study on PNC1 transport activity we focused on the trafficking of thymidine nucleotides. Their flux between cytosol and mitochondria can be carefully studied by employing proliferating cell cultures proficient or deficient of the cytosolic thymidine kinase TK1 and by incubating the cells with ^{3}H-thymidine for short periods of time, in order to monitor the intracellular flow of labelled thymidine nucleotides.

In TK1$^-$ cells the cytosolic salvage of TdR is non-functional and ^{3}H-TdR is only phosphorylated in mitochondria by TK2. When we label cycling cells with highly radioactive ^{3}H-TdR, the specific radioactivity of the mitochondrial dTTP (mtdTTP) is highly diluted (at least 40-fold) compared to the supplied ^{3}H-TdR, indicating that most mtdTTP is produced from unlabelled precursors (Fig. 1A). The main responsible for unlabelled dTTP synthesis is *de novo* ribonucleotide reduction in the cytosol, which is very active. This implies that the cytosolic unlabelled dTTP is then imported into mitochondria. RNR-dependent *de novo* synthesis is restricted to S-phase. In a cell population, the higher is the frequency of S-phase cells, the more active will be ribonucleotide reduction and the more diluted will be labelled dTTP inside mitochondria (Fig. 1A).
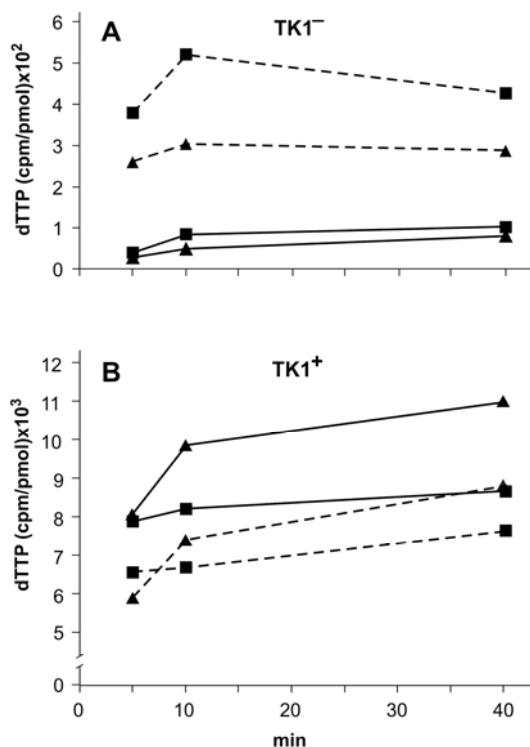

Fig. 1: Specific radioactivities of mt and cytosolic dTTP in TK1$^-$ and TK1$^+$ cells incubated with ^{3}H-TdR.
(A) Ost TK1$^-$ cells were incubated with 1 μM ^{3}H-TdR (20,000 cpm/pmol) for 5-40 min. After each time mt and cytosolic dNTP pools were separated and the specific radioactivities of the dTTP pools were measured by the DNA polymerase assay. (■), cultures with 22% S-phase cells; (▲), cultures with 33% S-phase. (B) HOS TK1$^+$ cells were incubated with 0.3 μM ^{3}H-TdR as above and mt and cytosolic dTTP pools were separated and analyzed. (■), cultures with 31% S-phase; (▲), cultures with 41% S. Dotted lines, mtdTTP. Continuous lines, cytosolic dTTP. Values are means of duplicate determinations. Notice the 10-fold difference in the scales of the ordinates.

Some radioactive dTTP is present also in the cytosol, meaning that the labelled thymidine nucleotides produced in mitochondria by phosphorylation of ^{3}H-TdR have been exported to the cytosol. The difference in specific radioactivity between the mitochondrial and the cytosolic thymidine phosphates indicates that the exported nucleotides are further diluted by non-radioactive nucleotides synthesized *de novo* (Fig. 1A).

In TK1$^+$ cells the cytosolic salvage of thymidine is active and ^{3}H-TdR is rapidly phosphorylated by TK1. The cytosolic dTTP pool becomes highly radioactive, with less than a 3-fold dilution of the specific radioactivity compared to the supplied ^{3}H-TdR (Fig.1B). This indicates that in TK1$^+$ cells the cytosolic salvage of thymidine heavily contributes to dTTP synthesis. TK1 is induced in S-phase and cultures with higher frequency of S-phase cells display a higher specific radioactivity of cytosolic dTTP. The specific radioactivities of the cytosolic and mitochondrial dTTP reach similar values and are similarly affected by the frequency of S-phase cells (Fig. 1B), indicating that labelled thymidine nucleotides are mostly produced in the cytosol by TK1-dependent salvage of ^{3}H-TdR and subsequently imported into mitochondria.

Thus, TK1$^+$ and TK1$^-$ cells are useful tools to investigate the direction of the transport of thymidine nucleotides across the inner mitochondrial membrane.

We study the function of PNC1 and the other putative mitochondrial transporter SLC25A36 in intact cells, where the carriers operate in their natural milieu and are exposed to physiological concentrations of nucleotides.

In order to understand if PNC1 participates in the trafficking of thymidine nucleotides described above, we modified the expression of the carrier by RNA interference or by inducible overexpression. PNC1 was stably downregulated through shRNAs or transiently silenced by siRNA transfection in Ost TK1$^-$ cells. In some experiments we combined stable PNC1 downregulation with transient SLC25A36 siRNA transfection in order to ascertain if the two proteins have overlapping transport activities and SLC25A36 can compensate for PNC1 downregulation. Silencing was effective under all conditions and reduced the mRNAs coding for the two proteins to 3-20% residual level (Fig. 2A).

The expression of PNC1 is low in Ost cells and in other cell lines [34] and we cannot monitor the disappearance of the endogenous protein by immunoblotting. This technique enables instead to follow the inducible overexpression of PNC1. The expression of the carrier was upregulated through the ecdyson receptor system [63, 64], which allows a ponasterone-inducible modulation of protein expression. In Ost TK1$^-$ and HEK293 TK1$^+$ the levels of PNC1 mRNA and protein increased with the dose of the inducer and the time of induction (Fig. 2B).

A

Silencing conditions	Mean % silencing ± SEM	
	PNC1	SLC25A36
33 shRNA	79.7 ± 1	
33 siRNA	86.1 ± 1.8	
33 shRNA + 36 siRNA	80 ± 2.6	97.2 ± 0.6
36 siRNA		91.4 ± 6.2

B

	48 h			72 h			
	NI	1	4	NI	1	4	
HEK293							PNC1
							UQCRFS1
protein	1	3.1	6.4	1	4.6	11.4	
mRNA	1	1.3	6.8	1	2.4	10.3	
Ost							* ←PNC1
protein	1	2.4	12.3	1	10.7	21.6	
mRNA	1	4.6	8.8	1	5.2	16.1	

Fig. 2: Manipulation of PNC1 expression by RNA interference or inducible overexpression in cultured human cells.
(A) Silencing of PNC1 alone or in combination with SLC25A36 in Ost cells was estimated from the residual level of the mRNAs measured by reverse-transcription real-time PCR. Stable PNC1 silencing is designated with 33shRNA; transient PNC1 or SLC25A36 silencing is designated with 33 or 36 siRNA. Values are the mean silencing levels obtained in all the experiments (5-2) performed under each condition ± SEM. (B) Cultures of HEK293 and Ost cells with inducible overexpression of PNC1 were incubated for 48 and 72 h with 0 (NI), 1 or 4 μM ponasterone. In HEK293 immunoblots the ubiquinol cytochrome C reductase (UQCRFS1) is used as a loading control, while in the Ost immunoblots an unspecific band (marked by the asterisk) is used for the normalization. Signal intensities were measured by ImageJ software. The relative increases of PNC1 mRNA were measured in parallel cultures as in (A) and are indicated under the blots.
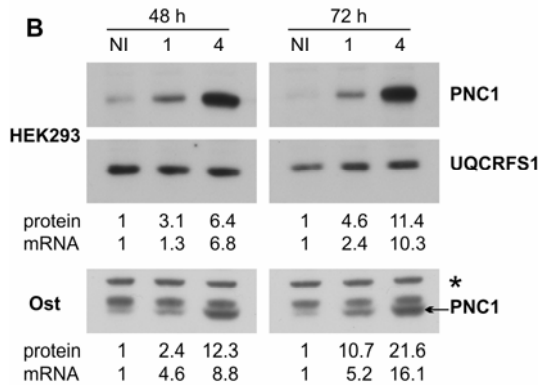
Graded overproduction of PNC1 did not modify the cell-cycle distribution of HEK293 cells but reduced progressively the frequency of S-phase cells in Ost cultures, thus affecting the concentrations of deoxynucleotides [63]. Therefore we could only use the overproducing HEK293 cells to study the effect of PNC1 overexpression (see below).

We demonstrate the efficiency of the downregulation at the protein level by showing that PNC1-silenced cells manifested the expected reduced import of uridine phosphates into mitochondria (see Fig. 4A). In our experiments we compare cell populations with a similar frequency of S-phase cells. Thus, the alterations in dNTP pool sizes and dynamics measured by us can be ascribed to PNC1 manipulation rather than to differences in proliferation rates.

Differently from published data [34], stable downregulation of PNC1 in Ost TK1⁻ cells did not produce a preferential depletion of pyrimidine nucleotides in mitochondria. While the cytosolic pools were unchanged (Fig. 3C), we measured a decrease of all mitochondrial ribo- and deoxyribonucleoside triphosphates in silenced cells (Fig. 3A). Normalization of the mt pools by their ATP content eliminated the differences between silenced and control cells (Fig. 3B).
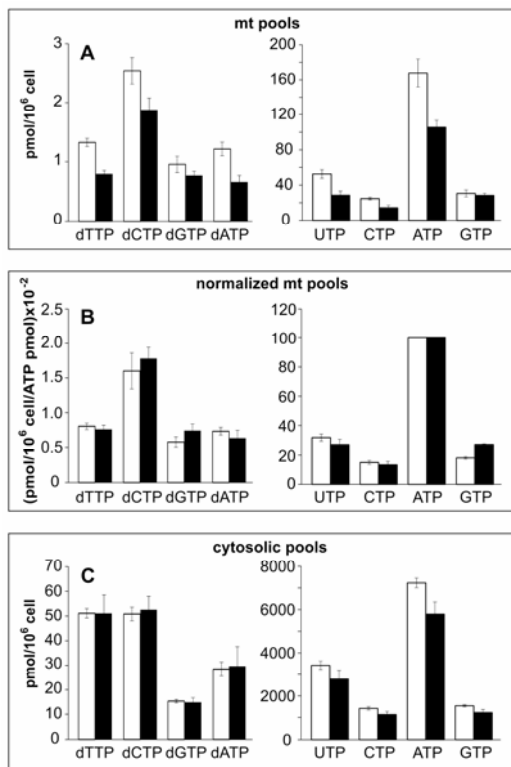
Fig. 3: **Stable downregulation of PNC1 in Ost cells reduces the concentration of deoxy- and ribonucleoside triphosphates in the mitochondrial pool without causing pool imbalance**.

Mitochondrial (A and B) and cytosolic (C) nucleotide pools were separated from 3 clones of Ost cells expressing an anti-PNC1 shRNA and 5 control clones transfected with the empty vector. Deoxynucleotides were measured by the DNA polymerase assay and ribonucleotides by HPLC. In (B) mt pool sizes of each sample were normalized by its mt ATP content. Black bars, silenced clones. White bars, controls. Values are means $\pm$ SEM.

This discrepancy with the previously published data may be explained considering that a prolonged PNC1 downregulation could overshadow changes in pool dynamics that may be detectable by labelling experiments.

We pulsed the cells with ^{3}H-uridine (UR) for 2-10 min, we then separated mt and cytosolic pools and measured the total radioactivity of uridine phosphates. Downregulation of PNC1 decreased the total radioactivity in mt pool; downregulation of SLC25A36 had no effect and silencing of both transporters resulted in the same picture we obtained for PNC1 downregulation (Fig. 4A). Although alterations of mtUTP were not detectable by pool size determination (Fig. 3B), the flow of radioactive uridine nucleotides from the cytosol into mitochondria revealed the effect of PNC1 silencing and demonstrates the downregulation of the carrier at the protein level.

Inducible overexpression of PNC1 in HEK293 cells caused an expansion of mtUTP pool size, passing from 14 $\pm$ 1.9 (mean $\pm$ SEM) pmol/10[6] non-induced cells to 29 $\pm$ 4.4 after induction with 4 µM ponasterone. Cytosolic pool sizes were unaffected. Moreover, PNC1 overexpressing HEK293 cells incubated with ^{3}H-UR contained more radioactivity in mitochondria than the controls (Fig. 4B), indicating an increased import of uridine nucleotides from the cytosol. Therefore, lowering or increasing the expression of PNC1 produced opposite effects on the import of uridine phosphates, in agreement with earlier data [34].
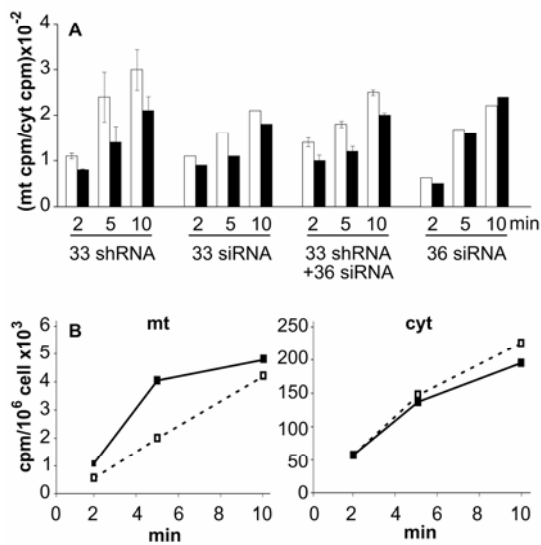
Fig. 4: Downregulation or overproduction of PNC1 cause opposite changes in the total radioactivity of uridine phosphates in the mitochondrial pool.
(A) In Ost cells PNC1 and SLC25A36 were silenced together or separately. Stable PNC1 silencing is designated with 33shRNA; transient PNC1 or SLC25A36 silencing is designated with 33 or 36 siRNA. Cells were incubated for 2-10 min with 0.1 µM ^{3}H-UR. The radioactivity in the mitochondrial pool was normalized by the corresponding cytosolic radioactivity. Black bars: silenced cells. White bars: controls. The experiments with stable shRNA-expressing clones were repeated twice; the range of variation is shown. (B) HEK293 cells were induced to overexpress PNC1 by 4 µM ponasterone and were incubated for 2-10 min with 0.1 µM ^{3}H-UR. The radioactivity of uridine phosphates in the mitochondrial (left panel) and cytosolic pool (right panel) is shown. (■) induced cutures, (□) non-induced controls. Data from one representative experiment. Notice the different scales of the ordinates for mt and cytosolic (cyt) pools.

To examine if PNC1 is involved in the rapid exchange of thymidine nucleotides across the mt membrane, we started our investigation in TK1$^-$ cells, which permit to study the export of thymidine phosphates from mitochondria when labelled with ^{3}H-TdR.

Ost TK1$^-$ cultures were silenced as in Fig 4A and labelled with ^{3}H-TdR for 5-40 min. In all experiments we controlled the degree of mRNA downregulation by real-time PCR and the frequency of S-phase cells. Only experiments in which the frequency of S-phase cells was nearly identical between silenced cultures and controls were considered. Under all conditions of PNC1 silencing, cytosolic dTTP pool size (Fig. 5B) and specific radioactivity (not shown) were not significantly affected, while in mitochondria a tendency for mtdTTP to decrease in size was evident (Fig. 5A). However, normalization of mtdTTP pool size by ATP content abolished the difference between transiently silenced and control cells (not shown). PNC1 knock-down produced instead a clear increase of the total and specific radioactivity (Fig. 5C) of the mtdTTP pool. This is attributable to the sole PNC1 because the combined downregulation of PNC1 and SLC25A36 did not change the picture and silencing of SLC25A36 alone had no effect.
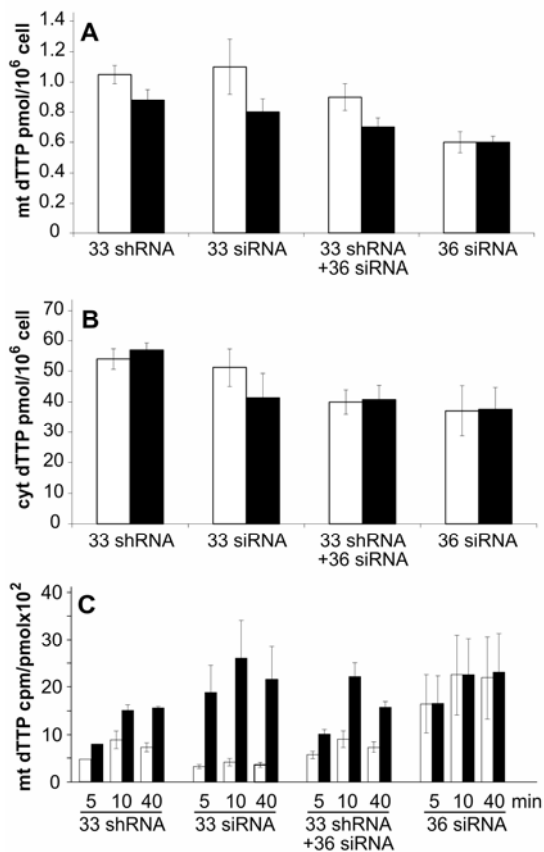
Fig. 5: Size and specific radioactivity of mitochondrial dTTP pools and size of cytosolic dTTP pools in Ost TK1⁻ cells with downregulation of PNC1 alone or in combination with SLC25A36 during labelling with 1 μM ³H-TdR.

Stable PNC1 silencing is designated with 33shRNA; transient PNC1 or SLC25A36 silencing is designated with 33 or 36 siRNA. After 5-40 min pulses with ³H-TdR mitochondrial and cytosolic nucleotide pools were extracted. The size of dTTP pools (A and B) and mtdTTP specific radioactivities (C) were measured by the DNA polymerase assay. In each experiment the mean size of the mt (A) or cytosolic (B) dTTP pool at the 3 times of TdR pulse was calculated. (C) specific radioactivities of mtdTTP in each series of silenced cultures at each time point during the pulse. Black bars, silenced cells. White bars, controls. Values are means ± SEM of 2-3 experiments per condition.

The higher specific radioactivity of mtdTTP in PNC1-silenced cells indicates that ³H-TdR is phosphorylated in mitochondria by TK2 and the radioactivity is retained in the organelle because of a lower export of thymidine phosphates.

We calculated the rate of mtdTTP export in control and silenced cells, as shown in Table 1 for one representative experiment. We based our calculations on the assumption that the three thymidine nucleotides are at isotopic equilibrium in mitochondria and by measuring the specific radioactivity of mtdTTP we estimate the dynamics of the whole mt pool of thymidine phosphates; we include all thymidine phosphates under the designation "dTTP export". In the cytosol dTTP corresponds to 85-90% of the total thymidine phosphates and we can assume it represents the whole cytosolic pool.

During 30 min of ³H-TdR incubation (i.e. between 10 and 40 min in the experiment described in Fig. 5C) we can calculate the total radioactivity counts that have left mitochondria by summing the increase of radioactivity in the cytosolic dTTP pool and the radioactivity incorporated into DNA. Although the total radioactivity exported is similar in control and silenced cells, the specific radioactivity of mtdTTP is higher in silenced cells and consequently the pmoles exported are less.

In our calculations the rate of DNA synthesis is a key factor. We did not consider those experiments where the rate of DNA synthesis is lower in silenced cells compared to control cells, because in that case a lower rate of mtdTTP export could simply reflect a lower consumption of DNA precursors rather than inhibition of dTTP transport.

The mean rate of dTTP export from mitochondria under all the conditions of PNC1 silencing tested in Fig. 5 was 0.40 ± 0.04 pmol/min (mean ± SEM) compared to a rate of 1.17 ± 0.23 in the controls (p<0.02). Thus, the isotope-flow methodology reveals alterations of mtdTTP dynamics that were not detectable by the simple determination of pool size and lead to the conclusion that PNC1 exports thymidine nucleotides, most likely dTTP, from mitochondria into the cytosol.

Table 1: Quantitation of dTTP export from mitochondria of control and PNC1-silenced Ost TK1⁻ cells incubated with ³H-TdR. Data come from a representative experiment in Fig. 5. All values are referred to one million cells.

Radioactivity flow during 30 min of ³H-TdR incubation	Control	PNC1-silenced
cyt dTTP cpm[a]	3010	2940
DNA cpm[b]	9740	11820
Total cpm exported from mitochondria	12750	14760
mean sp. radioactivity of mtdTTP	535	1457
pmol mtdTTP exported/min[c]	**0.79**	**0.34**
mean sp. radioactivity of cyt dTTP	86	81
DNA synthesis (pmol/min)[d]	3.8	4.9

[a] Increase of cytosolic dTTP radioactivity between 10 and 40 min of incubation with ³H-TdR. All values refer to the same time-window.
[b] Radioactivity incorporated into DNA.
[c] pmol of mtdTTP exported/min, calculated by dividing the total cpm exported from mitochondria by the mean specific radioactivity of mtdTTP.
[d] pmol of dTMP incorporated/min, calculated by dividing the counts incorporated into DNA by the specific radioactivity of cytosolic dTTP.

We then moved to TK1⁺ cells in order to investigate if PNC1 is involved also in the import of thymidine phosphates from cytosol into mitochondria. We upregulated the expression of PNC1 and pulsed the cells for 5-20 min with low concentrations of ³H-TdR.

Overexpression of PNC1 in TK1⁺ HEK293 cells produced almost a doubling of mtdTTP pool size (Fig. 6A) with only a small and transient increase in the specific radioactivity of mtdTTP (Fig 6B). In the overexpressing cultures the total radioactivity of the mtdTTP pool increased with the dose of the inducer (Fig. 6C). Thus, overexpression of PNC1 in HEK293 cells appears to have a small but reproducible positive effect on the import of thymidine phosphates into mitochondria.

In these experiments we cannot evaluate the rate of dTTP import into mitochondria because of the concomitant export of the radioactive nucleotides into the cytosol. The experiments with TK1⁺ cells do not allow to distinguish the

phosphorylation level of the imported nucleotide(s) because the interconversion among the three thymidine nucleotides occurs to rapidly to be detected at the time-scale of our experiments.
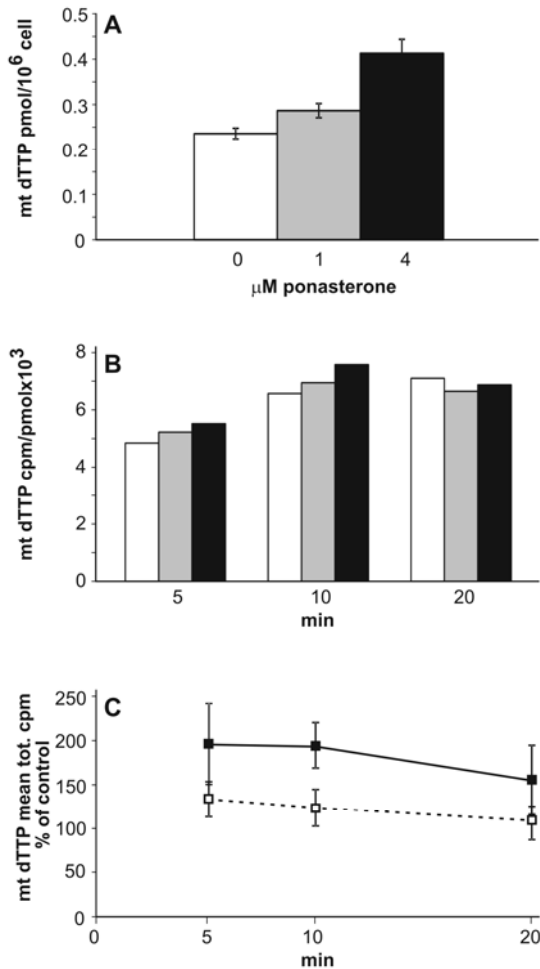

Fig. 6: Effects of PNC1 overexpression on the size and specific radioactivity of mtdTTP in HEK293 TK1$^+$ cells incubated with ^{3}H-TdR.
HEK293 cells were induced to overexpress PNC1 by incubation with 1 or 4 µM ponasterone for 72 h. (A) mean concentration of dTTP in the mitochondrial pools of controls (white bar) or cultures induced with 1 µM (gray bar) or 4 µM ponasterone (black bar). Values are means ± SEM from 4 experiments in which cells were pulsed with 0.05, 0.1, 0.3 or 1 µM ^{3}H-TdR for 5-20 min. The difference between controls and cultures induced with 4 µM ponasterone is highly significant (p<0.001) (B) specific radioactivity of mtdTTP in control and ponasterone-induced cultures pulsed with 0.3 µM ^{3}H-TdR; the color code is the same as in (A). (C) total radioactivity in the mtdTTP pools of cultures induced to overproduce PNC1 by 72 h incubation with 1 (□) or 4 (■) µM ponasterone, percent of non-induced controls. The range of the calculated values from 4 experiments is indicated. All samples induced with 4 µM ponasterone were significantly different (p<0.05) from the controls.

In order to investigate which phosphorylated species are imported by PNC1 we isolated mitochondria from control and PNC1 overexpressing cells and performed *in vitro* import assays.

In preliminary experiments we incubated isolated mitochondria for 2 min with ^{3}H-dTMP and monitored the import of the labelled nucleotide. ^{3}H-dTMP is rapidly and efficiently imported: at low (7-30 nM) external concentrations, it becomes 400- to 500-fold concentrated inside mitochondria. This increase is inversely related to the external concentration of the nucleotide. The properties of dTMP import reported here recapitulate what has already been described in

mitochondria isolated from mouse liver [26] (Fig. 7A). Overexpression of PNC1 does not enhance the rate of dTMP import (Fig. 7B).

We also monitored the transport of ^{3}H-dUMP and ^{3}H-dTTP (not shown). Upregulation of PNC1 does not affect the import into isolated mitochondria of any of the substrates we have analyzed.

At present we cannot exclude that PNC1 corresponds to the dTMP transporter functionally identified earlier [26]; further experiments with mitochondria isolated from PNC1-silenced cells are required.
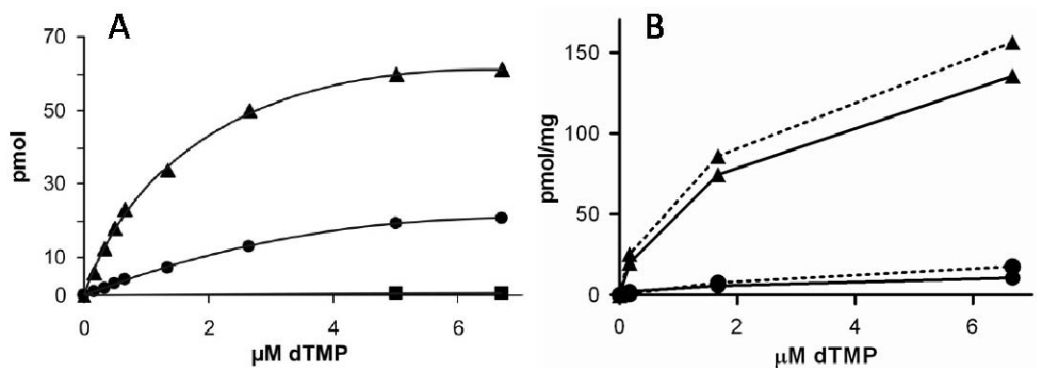
Fig. 7: Import of ^{3}H-dTMP into isolated mitochondria.
In (A) the import of ^{3}H-dTMP into isolated mitochondria from mouse liver is shown. Mitochondria were incubated with increasing concentrations of ^{3}H-dTMP (430 cpm/pmol) for 2 min and the amount of intramitochondria dTMP (▲), TdR (●)and dTTP+dTDP (■) was determined from their radioactivity. Data come from [26]. In (B) mitochondria were isolated from HEK293 cells induced to overexpress PNC1 by 72 h incubation with 4 µM ponasterone (dotted lines) or from non-induced controls (continuous lines). Isolated mitochondria were incubated with increasing concentrations of ^{3}H-dTMP (700 cpm/pmol) for 2 min. The pmoles of intramitochondrial dTMP (▲) and TdR (●) are normalized by the amount (mg) of mitochondria used during the *in vitro* transport assay. Data from one representative experiment are shown.

Our results show that PNC1 mediates the export of thymidine nucleotides and the import of uridine and thymidine nucleotides, but do not allow to distinguish the phosphorylation level of the transported nucleotides. The activity of SLC25A36, which is 60% identical to PNC1, remains unknown as its downregulation did not affect mt pools.

The present data agree with the published characterization of the substrate specificity of PNC1 [34], with the exception of the generalized moderate decrease of all mt ribo- and deoxyribonucleoside triphosphates in Ost cells after PNC1 silencing. At present we do not have an explanation for this decrease, considering that no differences in cell growth and cell size were detected between silenced Ost cells and controls.

We have succeeded in detecting the involvement of PNC1 in both import and export of thymidine phosphates by studying pool dynamics through short-term

isotope-flow experiments. Pool size determination *per se* instead did not permit to detect the effects of PNC1 manipulation. We can explain this observation by considering that the nucleotide carrier works within an enzyme network and that mitochondrial dNTPs are regulated by the interplay of synthetic and catabolic reactions [63, 66] and by exchange of precursors between mitochondria and cytoplasm. Thus, reduced or increased rates of bidirectional transport may be compensated by changes in intramitochondrial synthesis or degradation of thymidine nucleotides.

The export of thymidine nucleotides into the cytosol may be useful in non-cycling cells where TK2 is the only active thymidine kinase and thymidine salvage occurs inside mitochondria. The release of dTTP into the cytosol may be a way to complement the low constitutive *de novo* synthesis of dNTPs catalyzed by the R1/p53R2 ribonucleotide reductase [18, 71]. In cycling cells dTTP export from mitochondria continues even if its contribution to the cytosolic dTTP pool is marginal, probably because of the constitutive expression of the carrier, that is needed for the import of uridine phosphates, required for mtRNA synthesis [35].

4.2 Biochemical characterization and allosteric regulation of SAMHD1 enzymatic activity

The recently identified dNTP triphosphohydrolase SAMHD1 is allosterically activated by dGTP to degrade all four DNA precursors. Given its broad substrate specificity, this enzyme could represent the catabolic counterpart of RNR and could be similarly tightly regulated to maintain a balanced dNTP pool. This observation led us to investigate in depth the allosteric regulation of SAMHD1 activity. The data presented below mainly describe the biochemical properties of the mouse enzyme, but preliminary experiments suggest that a similar regulation exists for the human protein.

The recombinant mouse and human enzymes were expressed and purified as described under "Experimental Procedures". They were recovered as a single fraction enriched in a clean 75 kDa protein (Fig. 1A and 1C) with a dGTP-induced triphosphohydrolase activity: in the presence of dGTP, the purified enzymes were able to hydrolyze dATP to AdR. Our mouse SAMHD1 preparation has a higher hydrolase activity compared to published data [39], while the activity of the human enzyme agrees with previous measurements [41, 42, 72]. SAMHD1 is reported to be completely inactive in the absence of the allosteric effector dGTP [39, 40, 72]. However, our purified enzyme preparations display a basal dGTP-independent hydrolysis of the substrates which accounts for about 30% of the overall enzymatic activity (see Fig. 3). This basal degradation cannot be ascribed to contaminating phosphatases because it persists if the proteins are further purified by size-exclusion chromatography and intermediate degradation products (dADP and dAMP) were not detected by HPLC (Fig 1B and 1D).
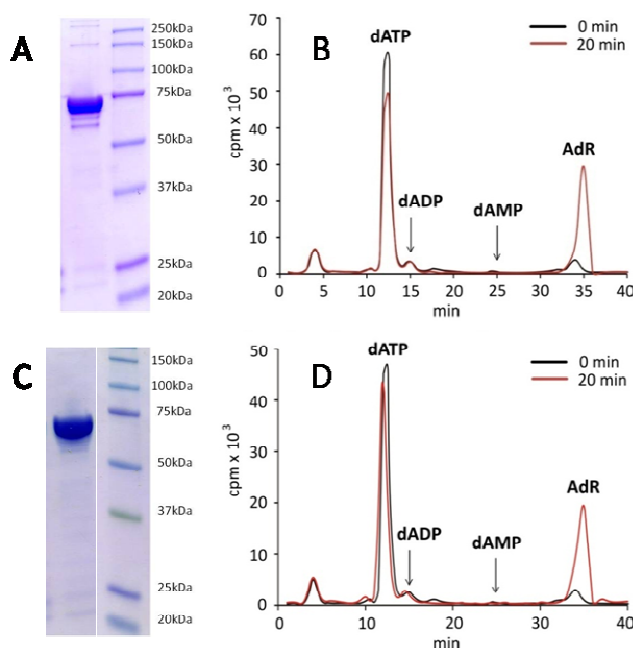

Fig. 1: Dephosphorylation of ^{3}H-dATP by purified mouse and human SAMHD1.
The purified fraction of mouse (A) and human (C) SAMHD1 consist in a clean 75 kDa band, as detected by Coomassie staining. The recombinant proteins (27 nM mouse SAMHD1 in B and 80 nM human SAMHD1 in D) were incubated with the substrate ^{3}H-dATP (100 µM) and the allosteric effector GTP (20 µM); the products of the reaction were analyzed by HPLC. The radioactivity chromatograms from 0-min (black) and 20-min (red) incubation are shown.

The enzymatic assay we set up to measure SAMHD1 activity is based on the use of labelled ^{3}H-dNTPs as substrates. The deoxynucleosides produced during the reaction are separated from unreacted deoxynucleotides and are quantified from their radioactivity. This method is highly sensitive: it detects even trace amounts of reaction products and allows to measure low levels of enzyme activity.

We first asked if any other (deoxy)nucleotide was able to activate SAMHD1 besides dGTP. We identified GTP as a potent activator of dATP hydrolysis while dGDP, dGMP, ATP, CTP, UTP were not as effective (not shown). We compared the ability of dGTP and GTP to stimulate ^{3}H-dATP hydrolysis by incubating the recombinant purified mouse SAMHD1 with increasing concentrations of the allosteric effectors (Fig. 2). dGTP is both an activator and a good substrate for the enzyme [40]: at low concentrations it stimulates ^{3}H-dATP hydrolysis but at increasing concentrations it competes with ^{3}H-dATP for the binding to the catalytic site until complete inhibition of ^{3}H-dATP degradation. On the contrary, GTP is not hydrolyzed by SAMHD1 as the ribose moiety is excluded from the catalytic site [42]. GTP and dGTP half-saturate the enzyme at a similar concentration, approximately 0.5 µM, but GTP is a more effective cofactor than dGTP because it stimulates SAMHD1 to hydrolyze ^{3}H-dATP at a higher rate.
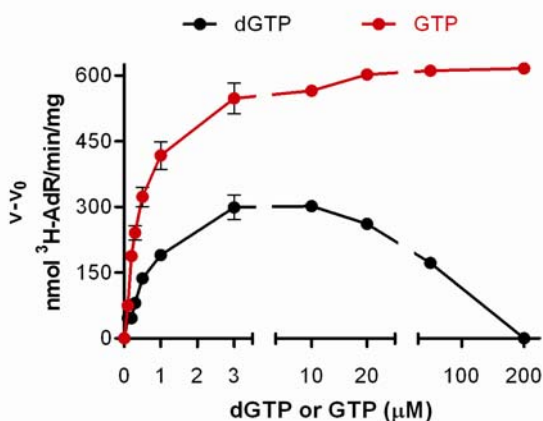

Fig. 2: GTP is a stronger activator of ^{3}H-dATP hydrolysis compared to dGTP.
Mouse SAMHD1 (13 nM) was incubated with the substrate ^{3}H-dATP (100 µM) and increasing concentrations (0-200 µM) of the allosteric effectors GTP (red) and dGTP (black). The rate of ^{3}H-dATP hydrolysis is expressed as specific activity (nmol ^{3}H-AdR/min/mg). It was calculated by subtracting the rate of substrate dephosphorylation in the absence of allosteric effectors (v_0) to that in the presence of allosteric effectors (v). Values are means of 3 experiments ± SEM.

While we were comparing the allosteric activation of SAMHD1 by dGTP and GTP, others have proposed that GTP serves as the primary activator of SAMHD1 in human cells [72]. We chose GTP as a cofactor in our experiments because it gives the advantage to separately analyze the catalytic activity and the regulatory mechanism of the enzyme. We measured the degradation of all four DNA precursors by mouse SAMHD1 (Fig. 3). Although ^{3}H-dGTP stimulates its own hydrolysis, GTP improves the degradation rate at low ^{3}H-dGTP concentrations

(Fig. 3C). GTP stimulates ^{3}H-dATP (Fig. 3A) and ^{3}H-dTTP (Fig. 3D) hydrolysis but it is scarcely effective in ^{3}H-dCTP degradation (Fig. 3B). Our data on substrate consumption best fit an allosteric sigmoidal distribution. The Hill coefficient is about 1.4 for all the substrates, which suggests a cooperative binding. The enzyme is approximately half-saturated in the presence of ≈ 200 μM ^{3}H-dATP and ^{3}H-dTTP or ≈ 100 μM ^{3}H-dGTP as substrates. Thus, its affinity for the allosteric effectors is at least 100 fold higher than the affinity for the substrates.
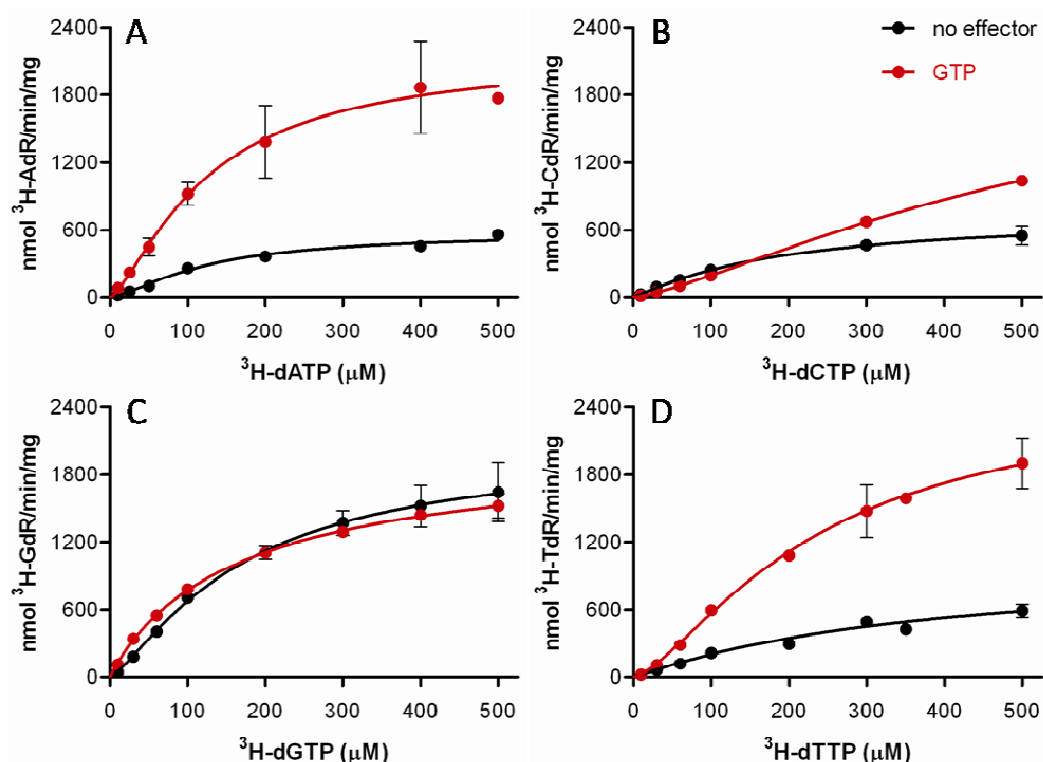
Fig. 3: Hydrolysis of ^{3}H-dNTPs by mouse SAMHD1.
Increasing concentrations (10-500 μM) of the substrates ^{3}H-dATP (A), ^{3}H-dCTP (B), ^{3}H-dGTP (C), ^{3}H-dTTP (D) were incubated with 8 nM (A) or 13 nM (B,C,D) mouse SAMHD1. We show the rate of substrate dephosphorylation (nmol ^{3}H-dN/min/mg) in the presence (red) or absence (black) of the allosteric effector GTP (20 μM). The data are fitted to the allosteric sigmoidal model; values are means of 2-5 experiments ± SEM.

We noticed that dTTP is poorly hydrolyzed in the physiological range of concentrations (0-60 μM) and that dCTP degradation is apparently non-existent in the 0-100 μM range. This observation suggested that the hydrolysis of the pyrimidine dNTPs could be improved by additional activators of SAMHD1 and we tried first to add a third nucleotide in the reaction mixture. We measured the effect of dATP, dTTP or dGTP addition on ^{3}H-dCTP hydrolysis in the presence or absence of the allosteric effector GTP. Among them, the combination dATP+GTP notably enhances the degradation of ^{3}H-dCTP, while the sole dATP behaves as

the no-effector control (Fig. 4B). The same combination of nucleotides also improves ^{3}H-dTTP consumption (Fig. 4D) and allows the enzyme to hydrolyze the four DNA precursors at comparable rates (Fig. 4). Thus, dATP is both a substrate and a cofactor for SAMHD1, similarly to dGTP. dATP is a secondary allosteric effector because it is able to stimulate the hydrolysis of the pyrimidine dNTPs only if combined with GTP, which can be then considered as the primary activator of SAMHD1.
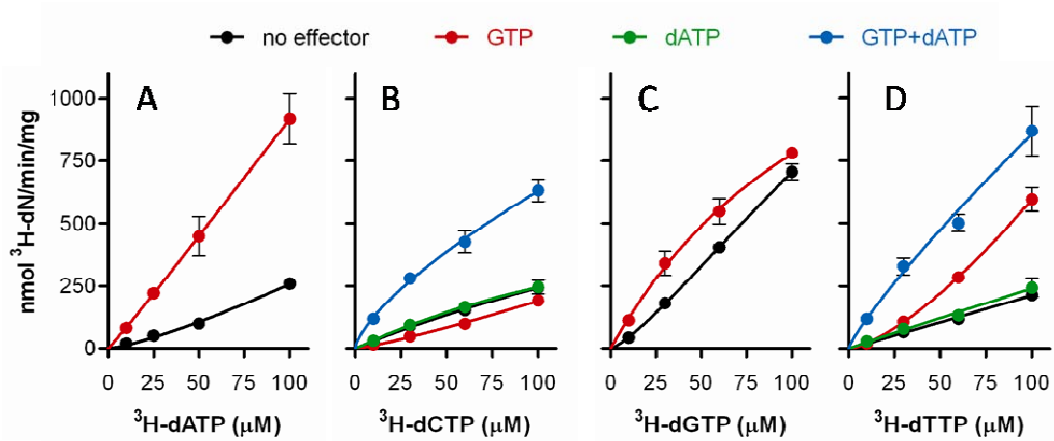

Fig. 4: dATP-induced hydrolysis of pyrimidine dNTPs shows that mouse SAMHD1 is able to degrade the four DNA precursors at comparable rates.
Increasing concentrations (10-100 µM) of the substrates ^{3}H-dATP (A), ^{3}H-dCTP (B), ^{3}H-dGTP (C), ^{3}H-dTTP (D) were incubated with 8 nM (A) or 13 nM (B,C,D) mouse SAMHD1. Data in A and C come from the same experiments described in Fig. 3A and 3C. We show the rate of substrate hydrolysis (nmol ^{3}H-dN/min/mg) in the presence of GTP (red), dATP (green), GTP+dATP (blue) or no effectors (black). The concentration of each allosteric effector is 20 µM. The four panels share the same scale on the ordinate. The data are fitted to an allosteric sigmoidal model; values are means of 2-5 experiments ± SEM.

To estimate the affinity of dATP for the allosteric site, we incubated the enzyme with the substrate ^{3}H-dCTP, the primary activator GTP and increasing concentrations of the secondary allosteric effector dATP (Fig 5). The curve follows an allosteric sigmoidal distribution with a Hill coefficient equal to 1.5.
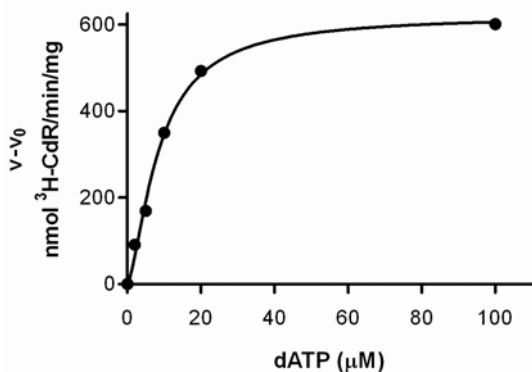

Fig. 5: Stimulation of ^{3}H-dCTP hydrolysis by dATP.
Mouse SAMHD1 (13 nM) was incubated with the substrate ^{3}H-dCTP (100 µM), the allosteric effector GTP (20 µM) and increasing concentrations (0-100 µM) of dATP. The rate of ^{3}H-dCTP hydrolysis (nmol ^{3}H-CdR/min/mg) was calculated as in Fig. 2, where v_0 is the rate of substrate dephosphorylation in the absence of dATP. The data are fitted to an allosteric sigmoidal model and derive from a single experiment. They have been confirmed using different substrate concentrations (10 and 30 µM ^{3}H-dCTP).

The curve also suggests that dATP has a preference for the allosteric site because ≈ 10 µM dATP is required by the enzyme to hydrolyze ^{3}H-dCTP at half of the maximum rate.

The secondary allosteric effector dATP could bind to the same site occupied by GTP. Alternatively, the existence of a secondary allosteric site could be hypothesized. If GTP and dATP share the same binding pocket, they will compete to gain access to it and exert their stimulatory function. We designed an experiment where we monitored ^{3}H-dCTP or ^{3}H-dTTP dephosphorylation induced by dATP in the presence of 20 or 500 µM GTP (Fig. 6). The stimulatory effect of dATP on both pyrimidine substrates was not inhibited by an increased concentration of GTP, which suggests that the two allosteric effectors are not competing for binding at the same allosteric site.
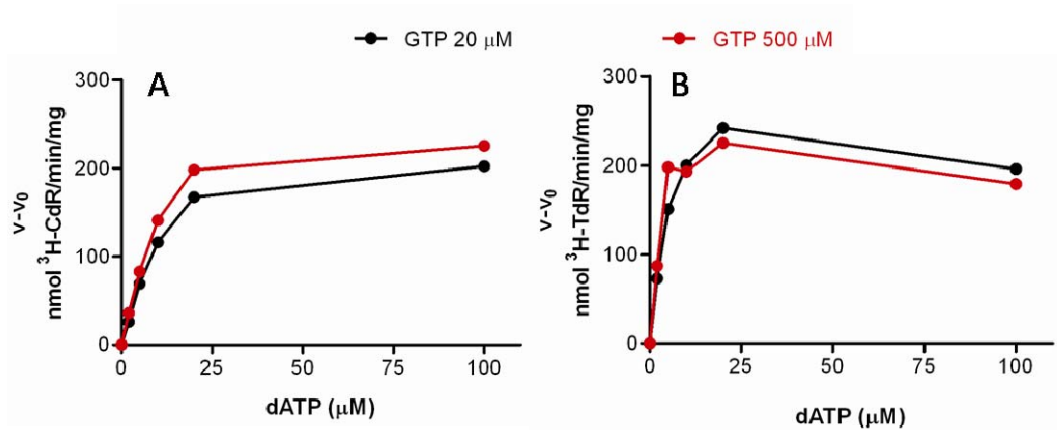

Fig. 6: The allosteric effectors GTP and dATP do not compete for the binding to the regulatory site.
Mouse SAMHD1 (13 nM) was incubated with the substrate ^{3}H-dCTP (A) or ^{3}H-dTTP (B) (both 30 µM), the allosteric effector GTP (20 µM in black, 500 µM in red) and increasing concentrations (0-100 µM) of dATP. The rate of substrate hydrolysis (nmol ^{3}H-CdR or ^{3}H-TdR/min/mg) was calculated as in Fig. 2, where v_0 is the rate of substrate dephosphorylation in the absence of dATP. The data derive from a single experiment, but have been confirmed using an additional substrate concentrations (10 µM ^{3}H-dCTP and ^{3}H-dTTP).

This result allows us to speculate that SAMHD1 harbours a distinct secondary site for the allosteric regulation of enzyme activity.

The conclusions we reached on the regulation of SAMHD1 enzymatic activity are not a prerogative of the mouse protein. Preliminary experiments indicate that a similar mechanism of regulation operates also for the human enzyme.

Human SAMHD1 differs from its mouse counterpart for some aspects: it is considerably more efficient in ^{3}H-dCTP hydrolysis (Fig. 7B) but the maximum degradation rate of the four ^{3}H-dNTPs is 3-4 fold lower (Fig. 7A-D). Despite these differences, we could confirm the additional regulatory role of dATP, which clearly enhances the degradation of ^{3}H-dCTP (Fig 7E), although it minimally affects ^{3}H-dTTP hydrolysis (Fig. 7F).
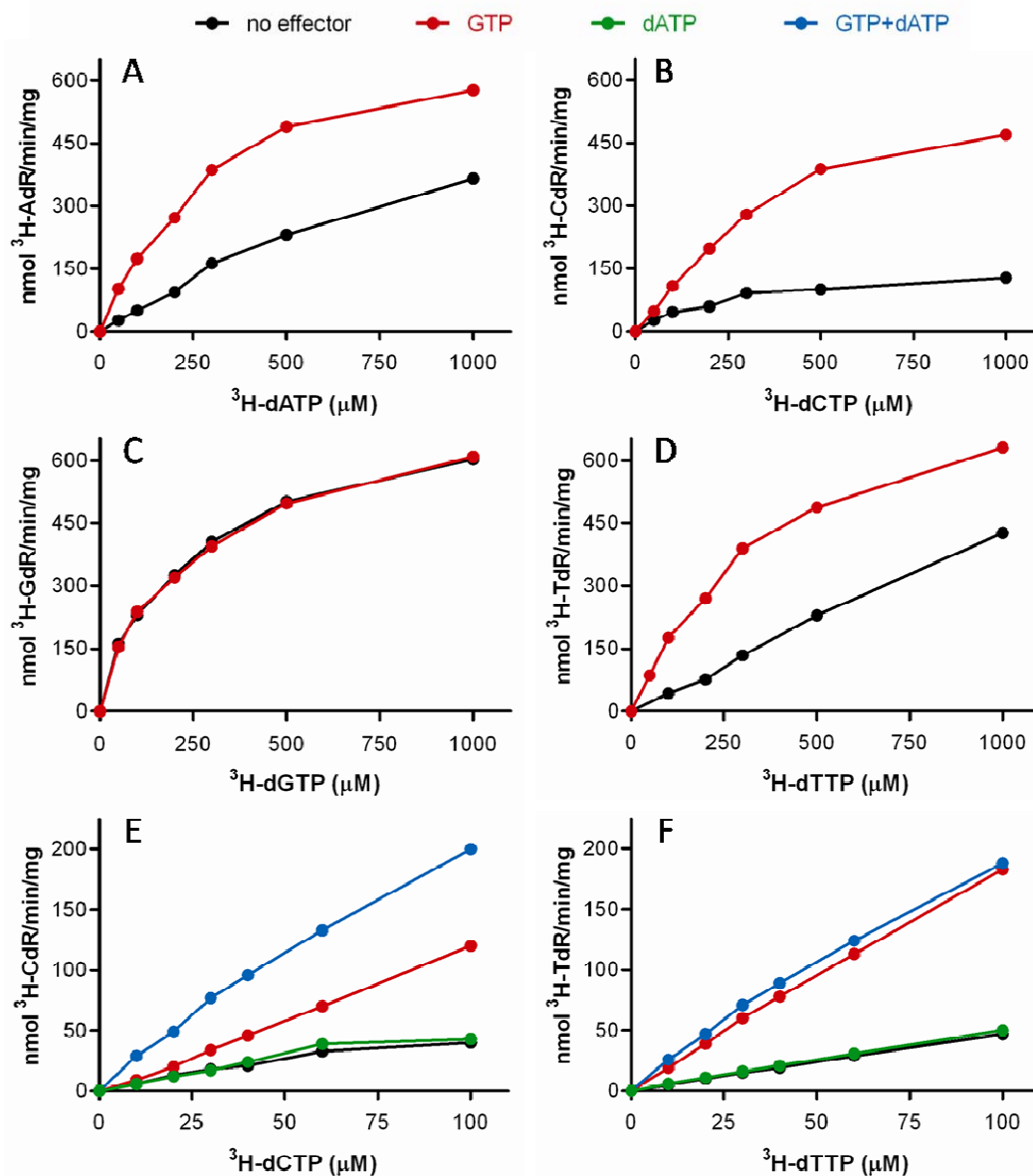
Fig. 7: Degradation of ^{3}H-dNTPs by human SAMHD1.
(A-D) Human SAMHD1 (40 nM) was incubated with increasing concentrations (50-1000 µM) of the substrates ^{3}H-dATP, ^{3}H-dCTP, ^{3}H-dGTP and ^{3}H-dTTP, respectively. A smaller concentration range (10-100 µM) is shown in E and F for the substrates ^{3}H-dCTP and ^{3}H-dTTP, respectively. We show the rate of substrate hydrolysis (nmol ^{3}H-dN/min/mg) in the presence of GTP (red), dATP (green), GTP+dATP (blue) or no effectors (black). The concentration of each allosteric effector is 20 µM. The data derive from a single experiment.

The intracellular concentration of dNTPs in human fibroblasts ranges from 10 to 60 µM in the proliferating state and becomes approximately 40-fold lower in the quiescent state (0.2-1.5 µM). These values have been derived from published data [19], assuming a volume of 2 µl for 10^6 cells. Our experiments mainly explore the concentration range typical of cycling cells. Under these conditions, there is a linear relationship between SAMHD1 activity and substrate

concentration, which makes SAMHD1 particularly sensitive to fluctuations in the pool of DNA precursors.

Two recent crystallographic structures of human SAMHD1 in complex with dGTP [42] or dGTP+dATP [73] provide a structural basis for our biochemical data demonstrating the existence of a second allosteric site. In the complex SAMHD1-dGTP, two dGTP molecules are located in each allosteric site. They interact differently with the surrounding residues: dGTP-1 is coordinated by several hydrogen-bonds involving the base moiety and is invariably detected in site-1, which is able to discriminate among the four bases and specifically accommodates guanine nucleotides; dGTP-2 is involved in less-specific interactions and can be substituted by dATP in site-2 when SAMHD1 is complexed with dGTP+dATP. Both allosteric sites are essential for SAMHD1 activity: mutagenesis of key residues constituting either site 1 or 2 abolishes tetramerization and dNTPase activity [42, 73]. Interestingly, a long α-helix connects the allosteric site-2 with the catalytic site [42]. Thus, site-2 could be a sensor of intracellular dNTP concentration regulating SAMHD1 activity and/or substrate specificity.

According to the available structural data, we can now give a better interpretation to our results: GTP and dATP do not compete because GTP binds to the primary site-1 and is likely excluded from site-2, while dATP only occupies the secondary site-2 and the enzyme is maximally active when both allosteric sites are occupied. Possibly, dCTP and dTTP could also bind to site-2 and participate in the regulatory mechanism modulating SAMHD1 activity, but further investigations at both a biochemical and a structural level are required.

A secondary allosteric site has just been reported in the SAMHD1-related dNTPase from *E. faecalis* [74]. The newly described pocket can accommodate each of the four dNTPs, which positively or negatively modulate enzyme activity.

Thus, the opposing reactions in dNTP metabolism catalyzed by RNR and SAMHD1 share a similar allosteric control based on two regulatory sites. The primary allosteric site determines the overall enzymatic activity and is highly selective: it specifically binds adenine nucleotides in the case of RNR or guanine nucleotides in the case of SAMHD1. The secondary allosteric site senses the intracellular concentration of dNTPs and interacts with different deoxynucleotides. It directs the substrate specificity of RNR and may have a similar function for SAMHD1.

A common regulatory mechanism based on allostery may be conserved from bacteria to humans to coordinate synthesis and degradation of the four dNTPs and ensure a balanced pool of DNA precursors.

4.3 The deoxynucleotide triphosphohydrolase SAMHD1 is a major regulator of DNA precursor pools in mammalian cells.

The main interest for SAMHD1 has so far been concentrated on the mechanism of its antilentiviral action. To us its presence in most mammalian organs and its deep evolutionary origin suggested a wider function for the enzyme than to be a guardian against viral infections.

SAMHD1 protein and mRNA are present in extracts from a variety of human cell lines (Fig. 1A). Monocytic THP1 cells have the highest SAMHD1 content and Jurkat T cells are negative. Non-transformed lung and skin fibroblasts show an intermediate expression of SAMHD1 and we chose these cells for our experiments. In proliferating cell extracts, SAMHD1 appears as a doublet (Fig. 1B), which may be explained by a post-translational modification, possibly phosphorylation by the cyclin A2/CDK1 complex [75]. The concentration of the protein changes considerably with cell proliferation, with confluent and quiescent fibroblasts containing much more SAMHD1 than cycling cells. By fluorescence microscopy we detected, in agreement with earlier work [43], SAMHD1 exclusively in the cell nucleus (Fig. 1C), in contrast to the known cytoplasmic location of proteins R1 and R2 [76, 77], the two subunits of RNR.
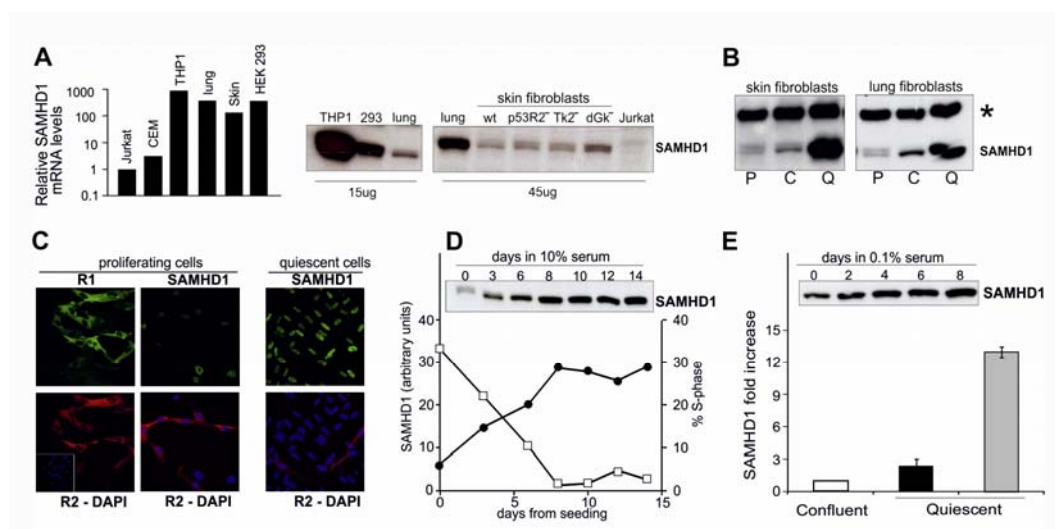

Fig. 1: Expression of SAMHD1 in cultured human cells.
(A) Relative levels of SAMHD1 mRNA and protein in different cell lines. The relative amount of mRNA was measured by real-time PCR in transformed cell lines (THP1, HEK293 and Jurkat) and in nontransformed lung and skin fibroblasts. SAMHD1 protein was detected by immunoblotting in extracts from transformed cells, lung and wild-type skin fibroblasts, and skin fibroblasts mutated for p53R3 or the mitochondrial thymidine (TK2) or deoxyguanosine (dGK) kinases. (B) Immunoblots of SAMHD1 from proliferating (P), confluent (C) and quiescent (Q) WT skin and lung fibroblasts. Asterisk marks an unspecific band (loading control). (C) Immunofluorescence shows nuclear localization of SAMHD1 (green) and cytosolic localization of the R1 (green) and R2 (red) subunits of RNR in lung fibroblasts. (D) Inverse relation between frequency of S-phase cells (open square) and abundance of SAMHD1 protein (filled circle) in proliferating cultures of lung fibroblasts. (E) Content of SAMHD1 in quiescent lung (black) and skin (gray) fibroblasts relative to the amount at confluency. The immunoblot shows the increasing SAMHD1 signal in lung fibroblasts.

The fluorescence signal of SAMHD1 is present in all cells, but its intensity varies markedly. In proliferating cells, a comparison with the S-phase specific R2 protein suggests an opposite regulation of SAMHD1 expression during the cell cycle: cells with a strong SAMHD1 signal are negative for R2, whereas cells with a strong R2 signal have only weak SAMHD1 fluorescence. The two proteins not only are present in separate cellular compartments but also are differently expressed during the cell cycle, with a major expression of SAMHD1 outside S-phase. Indeed, in cycling cultures with varying amounts of S-phase cells we found a clear inverse relation between the concentration of SAMHD1 and the frequency of S-phase cells. (Fig. 1D). In cultures of quiescent lung fibroblasts, all nuclei have a strong SAMHD1 signal (Fig. 1C) and immunoblotting analysis shows that SAMHD1 progressively accumulates in the cultures during serum starvation (Fig. 1E). So, the fluorescence data and the immunoblotting analysis suggest that the largest expression of SAMHD1 takes place outside S-phase and the enzyme degrades dNTPs mostly when DNA replication does not occur.

In order to study the participation of SAMHD1 in the enzymatic network regulating cellular dNTP concentrations, we manipulated protein expression through siRNAs. Transfection of cycling lung (Fig. 2) or skin fibroblasts (Fig. S1 in [78]) with anti-SAMHD1 siRNAs effectively depleted the cells of the mRNA in 24 h, whereas the protein declined more gradually. When after 48 h we transferred the silenced cells to new plates in siRNA-free medium, the mRNA reappeared after a lag of several days and the protein still later (Fig. 2).
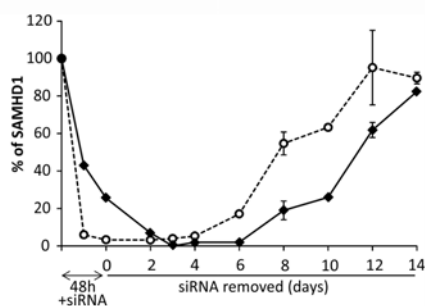

Fig. 2: Decline and recovery of SAMHD1 mRNA and protein during siRNA transfection and subsequent removal of siRNA.
Proliferating cultures of lung fibroblasts were transfected for 48 h with anti-SAMHD1 siRNA 24 h after seeding. Cells were then replaced in siRNA-free medium and grown for 14 d with medium changes every 3-4 d. SAMHD1 mRNA (open circle) and protein (filled diamond) were measured at the indicated times. Bars indicate range of values in two similar experiments.

During siRNA transfection the SAMHD1-silenced cultures grew more slowly than the nonsilenced controls, became growth-arrested at a lower density and contained fewer S-phase cells with a concomitant increase of G1 cells (Fig. 3A and 3B). To follow more closely the alteration of the cell cycle produced by the decline of SAMHD1, we pulsed cycling lung fibroblasts for 30 min with BrdU at different time points between 18 and 48 h of transfection with siRNA and determined the percentages of BrdU-positive S-phase cells by immunofluorescence (Fig. 3C). The frequency of positive cells in the control

cultures remained at around 30% at all time points. Instead, a small but significant decrease of S-phase cells was already apparent after 18 h of silencing and became stronger after 30 h, when the silenced cultures contained only half as many S-phase cells as the controls. Even an incomplete downregulation of SAMHD1 (Fig. 2) affects the progression of the cell cycle in non-transformed fibroblasts.
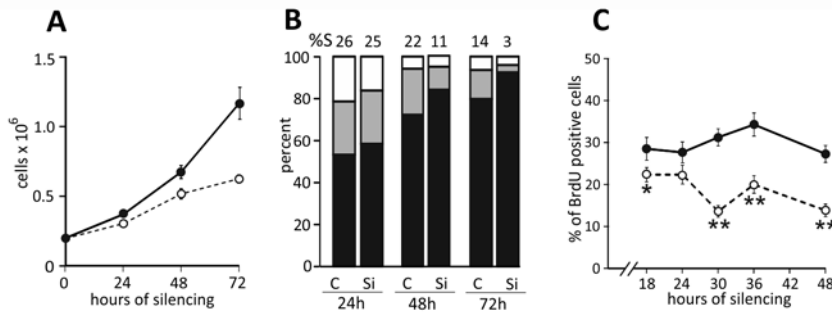

Fig. 3: Effect of SAMHD1 silencing on the growth of lung fibroblasts.
(A) Cell growth in cultures transfected for 24-72 h with anti-SAMHD1 (open circle) or control (filled circle) siRNAs. Data from three experiments. Bars are SEs. (B) Percent of G1 (black), S (gray) and G2/M (white) cells in transfected cultures. The frequency of S-phase cells is indicated above each control (C) and silenced (Si) sample. (C) Frequency of BrdU-positive cells in cultures transfected with control (filled circle) or anti-SAMHD1 (open circle) siRNAs for 18-48 h and incubated with BrdU during the last 30 min. Data are from two identical experiments. At least 500 cells were scored for each time point. The frequencies were compared by 2 x 2 χ^2 analysis. *P<0.05; **P<0.001. Bars are SEs.

In proliferating cell populations, the concentrations of the four dNTPs depend on the frequency of S-phase cells in which ribonucleotide reductase is strongly induced [7]. During the silencing experiments, the growing control cultures became progressively more crowded and their percentage of S-phase cells declined (Fig.3A and 3B). Accordingly, also the size of the dNTP pools declined, with dGTP always representing the smallest pool (Fig. 4). In SAMHD1-silenced cultures S-phase cells decreased faster than in the controls (Fig. 3B), but the dNTP pools did not show a corresponding decrease.

In Fig. 4 we transfected lung fibroblasts with two different anti-SAMHD1 siRNAs or control siRNA and during silencing related pool sizes to the frequency of S-phase cells, which reached the lowest value after 72 h of transfection. In the silenced cultures the progressive loss of SAMHD1 and S-phase cells stabilized the pools, interfering with their normal cell-cycle-dependent downregulation outside S-phase (Fig. 4). Similar results were obtained by silencing SAMHD1 in proliferating WT skin fibroblasts (Fig. S2 in [78]).
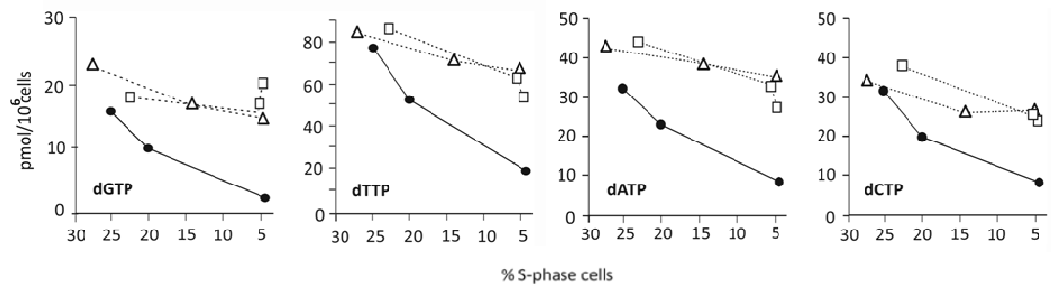
Fig. 4: Effect of SAMHD1 silencing on dNTP pools of cycling lung fibroblasts.
Relation between dNTP pool sizes and loss of S-phase cells in cycling cultures during transfection with two separate anti-SAMHD1 siRNAs (open square, open triangle) or with control siRNA (closed circle).

These data suggest that SAMHD1 expression, dNTP pool regulation, DNA synthesis and cell cycle progression are tightly interrelated: if we interfere with the regulation of SAMHD1 expression, we disrupt the cell-cycle-dependent regulation of dNTP pools and interfere with cell cycle progression, by disturbing the G1/S transition. A critical role is evident for SAMHD1 in keeping the pools low outside S-phase, when the cells are not replicating their nuclear DNA. A similar role has not been attributed to any other catabolic enzyme. As an example, downregulation of 5'-deoxynucleotidases, which contribute to the balance of dNTP pools and are constitutively expressed, does not produce significant alterations of nucleotide pool sizes [63, 79].

In proliferating cells, the ratios between the dNTP pools of silenced and control cells increases (Fig. 5A), especially for the dGTP pool. This can be ascribed to a slower decay of the dNTPs in the absence of SAMHD1 rather than to a real accumulation of dNTPs (see Fig. 4).
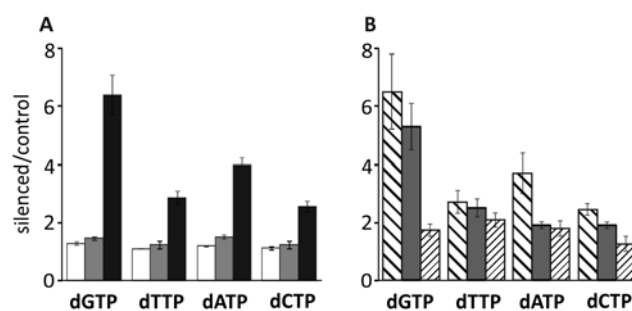

Fig. 5: Ratios between pool sizes of SAMHD1-silenced and control lung fibroblasts.
(A) Proliferating cultures transfected for 24 (white), 48 (gray) or 72 (black) h with control or anti-SAMHD1 siRNAs. Data are from three independent experiments. (B) Quiescent cultures of lung (broad stripes), WT (gray) or p53R2-mutated (thin stripes) skin fibroblasts transfected for 10 d with siRNAs during serum starvation. Data are from four to six experiments per cell line. All bars are SEMs.

Control lung fibroblasts, WT skin fibroblasts and p53R2-mutant skin fibroblasts [80] were made quiescent by serum starvation. These cultures contained less than 3% S-phase cells and after transfection with SAMHD1 siRNAs retained less

than 10% mRNA and only minimal SAMHD1 protein. Similarly to proliferating cells, in quiescent lung and WT skin fibroblasts the loss of SAMHD1 increases the sizes of the four dNTP pools and modifies their relative proportions, with a larger expansion of the dGTP pool (Fig. 5B). The p53R2-mutant cells behaves differently from the WT skin fibroblasts, as a similar increase in pool sizes does not occur. The differences are highly significant for dGTP (P<0.01), less significant for dCTP (P<0.05) and not significant for dATP and dTTP. Thus, in quiescent cells p53R2-dependent ribonucleotide reduction has a key role in the synthesis of DNA precursors [17, 18] and together with SAMHD1 is involved in a continuous turnover of dNTP pools.

It is interesting that both in growing and resting cells the main change caused by SAMHD1 knockdown concerns the dGTP pool, which is normally the smallest pool [63, 69]. These results reflect the preference of SAMHD1 for dGTP as a substrate and suggest that under normal conditions the small dGTP pool size may be due to a more efficient catabolism by SAMHD1 rather than to a low dGTP synthesis by ribonucleotide reduction. Considering that dGTP acts as an allosteric effector of both RNR and SAMHD1, the restraint operated by the latter enzyme on dGTP concentration may have interesting and still unidentified regulatory implications for both enzymes. A tight control of dGTP pool may be relevant for different physiological functions, as the recently reported case of telomere length homeostasis [81].

How fast do SAMHD1-silenced fibroblasts regain balanced dNTP pools and normal growth after removal of the siRNA? Following 48 h silencing of SAMHD1, we replated the cells at low density in fresh medium lacking siRNAs and continued the incubation for 12-14 d.
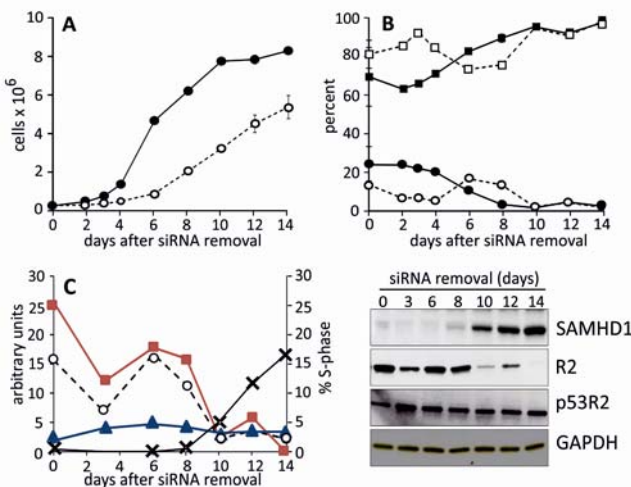

Fig. 6: Slow recovery of growth and cell cycle progression in lung fibroblasts after SAMHD1-silencing.

(A) Cell growth of control (filled circle) and SAMHD1-silenced (open circle) lung fibroblasts replated in siRNA-free medium after 48 h transfections. (B) Frequencies of G1- (squares) and S-phase (circles) cells in control (filled square, filled circle) and silenced (open square, open circle) cultures. Bars in A and B show range of values at identical time points in two independent experiments. (C) Abundance of SAMHD1 (x), R2 (filled square) and p53R2 (filled triangle) at the indicated days of culture without siRNA. Left reports in arbitrary units the quantification of the immunoblots on the right. Notice the parallelism between R2 expression and frequency of S-phase cells (open circle) in the cultures.

During this period, the control lung fibroblasts restarted their growth, with the highest percentage of S-phase cells immediately after seeding. The growth of the silenced cells remained strongly inhibited for 4-6 d (Fig. 6A), with a peak of S-phase cells appearing around 6 d from the start of the recovery period (Fig. 6B). In skin fibroblasts, the silencing caused a similar growth delay and a small peak of S-phase cells after 6 d (Fig. S3 in [78]).

Both cell lines had the capacity to resume growth after removal of siRNA, but only after an extended lag phase. The long lag period paralleled the slow recovery of SAMHD1 mRNA and protein after the shift to siRNA-free conditions (Fig. 2 and Fig. 6C) and was probably due to the stability of the siRNA internalized by the cells during the 48 h transfection. During the recovery period, the pattern of R2 variations coincided with that of S-phase cells, whereas p53R2 was more stable.

We determined the effect of siRNA removal on the size of the dNTP pools in both lung and skin fibroblasts. In both cases there was a nearly identical dramatic pool increase in all four pools, with a peak at the third to sixth day of recovery (Fig. S4 in [78]), when the cells contained some SAMHD1 mRNA but SAMHD1 protein had not yet returned. The dNTP peaks coincided in time with a small peak of S-phase cells (Fig. 6B).

The two cell lines showed highly similar behaviour both for the timing of pool changes and for their increases. We therefore combined the results and divided the average pool sizes of silenced and control cells to calculate the increase in size for each pool (Fig. 7). Most impressive is the peak value for dGTP after 6 d. At that point dGTP accounted for more than 20% of the total cellular pools, more than twice its percentage in a cycling cell population. When SAMHD1 at later times became available, the pool values normalized and cell growth resumed.
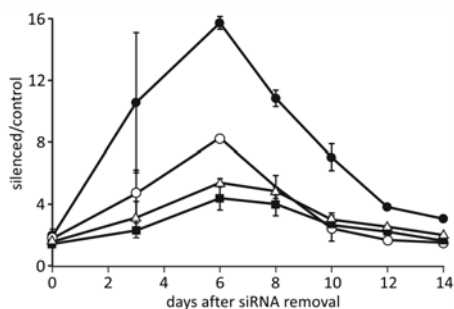

Fig. 7: Persistence of large dNTP pools in lung and skin fibroblasts after siRNA silencing of SAMHD1.
Mean ratios between sizes of dGTP (filled circle), dCTP (open circle), dTTP (filled square) and dATP (open triangle) pools in silenced and control cells during 14 d without siRNA. Data from experiments with lung fibroblasts and skin fibroblasts. Bars show range of values.

These results clearly demonstrate that SAMHD1 is not only required for the maintenance of normal-sized dNTP pools but also for their normal proportions. SAMHD1 prevents the overproduction of dNTPs and exerts its activity mostly outside S-phase.

The cell-cycle-related regulation of the enzyme minimizes its activity during S-phase when large quantities of dNTPs are required for DNA replication. These are supplied mainly by RNR, whose cell-cycle regulation is opposite to that of SAMHD1 and provides maximal activity during S-phase. The mechanism of cell-cycle regulation of SAMHD1 is not known at present. However, evidences for a transcriptional and post-translational control have recently been reported. SAMHD1 gene transcription is regulated by methylation and histone modifications [82]; the protein is phosphorylated at T592 residue [75, 83], which may represent a signal for ubiquitin-dependent degradation [84].

SAMHD1 removes in the nucleus a potentially dangerous surplus of DNA precursors during the G1 phase of the cell cycle. In budding yeast, constitutively high dNTP pools result in G1 delay, probably due to a disturbance in the loading of Cdc45, a component of pre-initiation complexes at the DNA replication origins [85]. In contrast to yeast experiments, our experiments were done with unsynchronized cell populations and we could not measure the pool alterations occurring specifically in G1 cells. Nevertheless, it appears likely that the downregulation of SAMHD1 affected the small G1 pools at an early stage and raised them enough to trigger the G1 arrest by a mechanism at present still undefined.

The extra-S phase activity of SAMHD1 fulfils two main functions: (i) during cell proliferation it maintains the G1 pools at the correct level for a regular transition into S, possibly through the normal assembly of the pre-initiation complexes and (ii) by lowering the dNTP pools, it deprives invading viruses of the necessary DNA precursors.

Mutations in SAMHD1 cause the Aicardi-Goutières syndrome, a genetic neurodegenerative disorder with an improper activation of the immune system [43], probably triggered by an abnormal metabolism of nucleic acids [86]. Other causative genes for this disease encode the 3'→ 5' exonuclease TREX1 and the RNASEH2 endonuclease complex [86]. An additional nuclease activity of SAMHD1 is still highly debated, with an early report excluding [40] and recent work supporting [70] this alternative function. SAMHD1 has also been implicated in the modulation of the LINE-1 autonomous retrotransposition [87].

The mechanism underlying the phenotype of the Aicardi-Goutières syndrome caused by SAMHD1 mutations is still unknown, but the occasional occurrence of mitochondrial DNA deletions [88] might be linked to dNTP pool abnormalities. Indeed, a regulated dNTP pool outside S-phase is important for the fidelity of DNA repair and mitochondrial DNA replication. The destabilizing effects of imbalanced dNTP pools on the nuclear and mitochondrial genomes are well known and exemplified by severe human diseases linked to genetic deficiencies of catabolic enzymes [56, 57, 60].

5.   CONCLUSIONS

This work underlines the key role of dNTP degradation in modulating the availability of DNA precursors during the cell cycle.

Intracellular dNTPs are present at a low basal level outside S-phase and expand when cells are committed to replicate their nuclear DNA. These oscillations in dNTP concentrations reflect the cell-cycle regulation of RNR expression and activity, which are restricted to S-phase. So far, *de novo* synthesis by RNR was considered to be the main mechanism regulating the intracellular concentration of dNTPs in the cell cycle.

We now describe an additional level of control, i.e. degradation by the recently characterized dNTP triphosphohydrolase SAMHD1. Our experiments show that SAMHD1 undergoes a cell-cycle dependent regulation opposite to that of RNR, with the largest expression outside S-phase. A new picture comes out, where the differential regulation of anabolic and catabolic enzymatic activities determines the intracellular fluctuations of dNTPs and the correct progression of the cell cycle. In S-phase dNTP pools are allowed to expand by up-regulation of RNR-dependent *de novo* synthesis and a concomitant inhibition of SAMHD1-mediated degradation. Outside S-phase *de novo* synthesis of dNTPs persists at a lower rate. In the absence of DNA synthesis, DNA precursors are not consumed; they would accumulate and disturb the G1/S transition. SAMHD1 prevents the expansion of dNTPs in G1 by continuously turning over the pool and allows the normal progression of the cell cycle.

An even more sophisticated regulation of SAMHD1 activity emerges from the combination of our biochemical characterization and the existing crystallographic data. Two distinct sites contribute to the allosteric control of SAMHD1 activity and substrate specificity. GTP is the primary activator inducing the hydrolysis of all four dNTPs; it binds to the primary allosteric site, which is specific for guanine nucleotides. The secondary allosteric site has apparently a broad specificity, it can accommodate dATP with a resulting enhancement of pyrimidine deoxynucleotide hydrolysis. This newly described allosteric site may endow the enzyme with the ability to sense the intracellular concentration of dNTPs and adjust its activity accordingly, in order to maintain pool balance.

The other major issue in this thesis concerns intracellular deoxynucleotide trafficking. Deoxynucleotides need to be exchanged between cytosol and mitochondria to integrate the metabolism of DNA precursors in the two compartments, that are separated by the impermeable inner mitochondrial membrane. This is particularly important in non-dividing cells, where the pathways for dNTP synthesis undergo profound rearrangements: the

contribution of the cytosolic *de novo* and salvage pathways is strongly reduced, while the intramitochondrial salvage of deoxynucleosides is up-regulated. The molecular nature of the carriers for dNTP transport has remained elusive for a long time. Here we have demonstrated in intact cells that the pyrimidine nucleotide carrier PNC1 is involved in the bidirectional trafficking of thymidine nucleotides across the inner mitochondrial membrane.

REFERENCES

[1] C. Rampazzo, C. Miazzi, E. Franzolin, G. Pontarin, P. Ferraro, M. Frangini, P. Reichard, V. Bianchi, Regulation by degradation, a cellular defense against deoxyribonucleotide pool imbalances, Mutat. Res. 703 (2010) 2-10.

[2] C.F. Woeller, D.D. Anderson, D.M. Szebenyi, P.J. Stover, Evidence for small ubiquitin-like modifier-dependent nuclear import of the thymidylate biosynthesis pathway, J. Biol. Chem. 282 (2007) 17623-17631.

[3] D.D. Anderson, C.M. Quintero, P.J. Stover, Identification of a de novo thymidylate biosynthesis pathway in mammalian mitochondria, Proc. Natl. Acad. Sci. U. S. A. 108 (2011) 15163-15168.

[4] J.D. Young, S.Y. Yao, J.M. Baldwin, C.E. Cass, S.A. Baldwin, The human concentrative and equilibrative nucleoside transporter families, SLC28 and SLC29, Mol. Aspects Med. 34 (2013) 529-547.

[5] Y. Lai, C.M. Tse, J.D. Unadkat, Mitochondrial expression of the human equilibrative nucleoside transporter 1 (hENT1) results in enhanced mitochondrial toxicity of antiviral drugs, J. Biol. Chem. 279 (2004) 4490-4497.

[6] V. Bianchi, J. Spychala, Mammalian 5'-nucleotidases, J. Biol. Chem. 278 (2003) 46195-46198.

[7] P. Reichard, Interactions between deoxyribonucleotide and DNA synthesis, Annu. Rev. Biochem. 57 (1988) 349-374.

[8] S. Bjorklund, S. Skog, B. Tribukait, L. Thelander, S-phase-specific expression of mammalian ribonucleotide reductase R1 and R2 subunit mRNAs, Biochemistry. 29 (1990) 5452-5458.

[9] Y. Engstrom, S. Eriksson, I. Jildevik, S. Skog, L. Thelander, B. Tribukait, Cell cycle-dependent expression of mammalian ribonucleotide reductase. differential regulation of the two subunits, J. Biol. Chem. 260 (1985) 9114-9116.

[10] A. Chabes, L. Thelander, Controlled protein degradation regulates ribonucleotide reductase activity in proliferating mammalian cells during the normal cell cycle and in response to DNA damage and replication blocks, J. Biol. Chem. 275 (2000) 17747-17753.

[11] A.L. Chabes, C.M. Pfleger, M.W. Kirschner, L. Thelander, Mouse ribonucleotide reductase R2 protein: A new target for anaphase-promoting complex-Cdh1-mediated proteolysis, Proc. Natl. Acad. Sci. U. S. A. 100 (2003) 3925-3929.

[12] V. D'Angiolella, V. Donato, F.M. Forrester, Y.T. Jeong, C. Pellacani, Y. Kudo, A. Saraf, L. Florens, M.P. Washburn, M. Pagano, Cyclin F-mediated degradation of ribonucleotide reductase M2 controls genome integrity and DNA repair, Cell. 149 (2012) 1023-1034.

[13] P.Y. Ke, Y.Y. Kuo, C.M. Hu, Z.F. Chang, Control of dTTP pool size by anaphase promoting complex/cyclosome is essential for the maintenance of genetic stability, Genes Dev. 19 (2005) 1920-1933.

[14] C.L. Li, C.Y. Lu, P.Y. Ke, Z.F. Chang, Perturbation of ATP-induced tetramerization of human cytosolic thymidine kinase by substitution of serine-13 with aspartic acid at the mitotic phosphorylation site, Biochem. Biophys. Res. Commun. 313 (2004) 587-593.

[15] P.Y. Ke, Z.F. Chang, Mitotic degradation of human thymidine kinase 1 is dependent on the anaphase-promoting complex/cyclosome-CDH1-mediated pathway, Mol. Cell. Biol. 24 (2004) 514-526.

[16] H. Tanaka, H. Arakawa, T. Yamaguchi, K. Shiraishi, S. Fukuda, K. Matsui, Y. Takei, Y. Nakamura, A ribonucleotide reductase gene involved in a p53-dependent cell-cycle checkpoint for DNA damage, Nature. 404 (2000) 42-49.

[17] P. Hakansson, A. Hofer, L. Thelander, Regulation of mammalian ribonucleotide reduction and dNTP pools after DNA damage and in resting cells, J. Biol. Chem. 281 (2006) 7834-7841.

[18] G. Pontarin, P. Ferraro, P. Hakansson, L. Thelander, P. Reichard, V. Bianchi, p53R2-dependent ribonucleotide reduction provides deoxyribonucleotides in quiescent human fibroblasts in the absence of induced DNA damage, J. Biol. Chem. 282 (2007) 16820-16828.

[19] G. Pontarin, P. Ferraro, L. Bee, P. Reichard, V. Bianchi, Mammalian ribonucleotide reductase subunit p53R2 is required for mitochondrial DNA replication and DNA repair in quiescent cells, Proc. Natl. Acad. Sci. U. S. A. 109 (2012) 13302-13307.

[20] E. Franzolin, C. Rampazzo, M.J. Perez-Perez, A.I. Hernandez, J. Balzarini, V. Bianchi, Bromovinyl-deoxyuridine: A selective substrate for mitochondrial thymidine kinase in cell extracts, Biochem. Biophys. Res. Commun. 344 (2006) 30-36.

[21] L. Leanza, P. Ferraro, P. Reichard, V. Bianchi, Metabolic interrelations within guanine deoxynucleotide pools for mitochondrial and nuclear DNA maintenance, J. Biol. Chem. 283 (2008) 16437-16445.

[22] T. Spasokoukotskaja, E.S. Arner, O. Brosjo, P. Gunven, G. Juliusson, J. Liliemark, S. Eriksson, Expression of deoxycytidine kinase and phosphorylation of 2-chlorodeoxyadenosine in human normal and tumour cells and tissues, Eur. J. Cancer. 31A (1995) 202-208.

[23] C.H. Chen, Y.C. Cheng, The role of cytoplasmic deoxycytidine kinase in the mitochondrial effects of the anti-human immunodeficiency virus compound, 2',3'-dideoxycytidine, J. Biol. Chem. 267 (1992) 2856-2859.

[24] G. Pontarin, L. Gallinaro, P. Ferraro, P. Reichard, V. Bianchi, Origins of mitochondrial thymidine triphosphate: Dynamic relations to cytosolic pools, Proc. Natl. Acad. Sci. U. S. A. 100 (2003) 12159-12164.

[25] E.G. Bridges, Z. Jiang, Y.C. Cheng, Characterization of a dCTP transport activity reconstituted from human mitochondria, J. Biol. Chem. 274 (1999) 4620-4625.

[26] P. Ferraro, L. Nicolosi, P. Bernardi, P. Reichard, V. Bianchi, Mitochondrial deoxynucleotide pool sizes in mouse liver and evidence for a transport mechanism for thymidine monophosphate, Proc. Natl. Acad. Sci. U. S. A. 103 (2006) 18586-18591.

[27] A. Bourdon, L. Minai, V. Serre, J.P. Jais, E. Sarzi, S. Aubert, D. Chretien, P. de Lonlay, V. Paquis-Flucklinger, H. Arakawa, Y. Nakamura, A. Munnich, A. Rotig, Mutation of RRM2B, encoding p53-controlled ribonucleotide reductase (p53R2), causes severe mitochondrial DNA depletion, Nat. Genet. 39 (2007) 776-780.

[28] F. Palmieri, The mitochondrial transporter family (SLC25): Physiological and pathological implications, Pflugers Arch. 447 (2004) 689-709.

[29] V. Dolce, G. Fiermonte, M.J. Runswick, F. Palmieri, J.E. Walker, The human mitochondrial deoxynucleotide carrier and its role in the toxicity of nucleoside antivirals, Proc. Natl. Acad. Sci. U. S. A. 98 (2001) 2284-2288.

[30] M.J. Lindhurst, G. Fiermonte, S. Song, E. Struys, F. De Leonardis, P.L. Schwartzberg, A. Chen, A. Castegna, N. Verhoeven, C.K. Mathews, F. Palmieri, L.G. Biesecker, Knockout of Slc25a19 causes mitochondrial thiamine pyrophosphate depletion, embryonic lethality, CNS malformations, and anemia, Proc. Natl. Acad. Sci. U. S. A. 103 (2006) 15927-15932.

[31] T. Haitina, J. Lindblom, T. Renstrom, R. Fredriksson, Fourteen novel human members of mitochondrial solute carrier family 25 (SLC25) widely expressed in the central nervous system, Genomics. 88 (2006) 779-790.

[32] C.M. Marobbio, M.A. Di Noia, F. Palmieri, Identification of a mitochondrial transporter for pyrimidine nucleotides in saccharomyces cerevisiae: Bacterial expression, reconstitution and functional characterization, Biochem. J. 393 (2006) 441-446.

[33] E. Van Dyck, B. Jank, A. Ragnini, R.J. Schweyen, C. Duyckaerts, F. Sluse, F. Foury, Overexpression of a novel member of the mitochondrial carrier family rescues defects in both DNA and RNA metabolism in yeast mitochondria, Mol. Gen. Genet. 246 (1995) 426-436.

[34] S. Floyd, C. Favre, F.M. Lasorsa, M. Leahy, G. Trigiante, P. Stroebel, A. Marx, G. Loughran, K. O'Callaghan, C.M. Marobbio, D.J. Slotboom, E.R. Kunji, F. Palmieri, R. O'Connor, The insulin-like growth factor-I-mTOR signaling pathway induces the mitochondrial pyrimidine nucleotide carrier to promote cell growth, Mol. Biol. Cell. 18 (2007) 3545-3555.

[35] C. Favre, A. Zhdanov, M. Leahy, D. Papkovsky, R. O'Connor, Mitochondrial pyrimidine nucleotide carrier (PNC1) regulates mitochondrial biogenesis and the invasive phenotype of cancer cells, Oncogene. 29 (2010) 3964-3976.

[36] L. Thelander, P. Reichard, Reduction of ribonucleotides, Annu. Rev. Biochem. 48 (1979) 133-158.

[37] P. Nordlund, P. Reichard, Ribonucleotide reductases, Annu. Rev. Biochem. 75 (2006) 681-706.

[38] S.J. Elledge, Z. Zhou, J.B. Allen, Ribonucleotide reductase: Regulation, regulation, regulation, Trends Biochem. Sci. 17 (1992) 119-123.

[39] R.D. Powell, P.J. Holland, T. Hollis, F.W. Perrino, Aicardi-goutieres syndrome gene and HIV-1 restriction factor SAMHD1 is a dGTP-regulated deoxynucleotide triphosphohydrolase, J. Biol. Chem. 286 (2011) 43596-43600.

[40] D.C. Goldstone, V. Ennis-Adeniran, J.J. Hedden, H.C. Groom, G.I. Rice, E. Christodoulou, P.A. Walker, G. Kelly, L.F. Haire, M.W. Yap, L.P. de Carvalho, J.P. Stoye, Y.J. Crow, I.A. Taylor, M. Webb, HIV-1 restriction factor SAMHD1 is a deoxynucleoside triphosphate triphosphohydrolase, Nature. 480 (2011) 379-382.

[41] J. Yan, S. Kaur, M. Delucia, C. Hao, J. Mehrens, C. Wang, M. Golczak, K. Palczewski, A.M. Gronenborn, J. Ahn, J. Skowronski, Tetramerization of SAMHD1 is required for biological activity and inhibition of HIV infection, J. Biol. Chem. (2013) .

[42] X. Ji, Y. Wu, J. Yan, J. Mehrens, H. Yang, M. DeLucia, C. Hao, A.M. Gronenborn, J. Skowronski, J. Ahn, Y. Xiong, Mechanism of allosteric activation of SAMHD1 by dGTP, Nat. Struct. Mol. Biol. 20 (2013) 1304-1309.

[43] G.I. Rice, J. Bond, A. Asipu, R.L. Brunette, I.W. Manfield, I.M. Carr, J.C. Fuller, R.M. Jackson, T. Lamb, T.A. Briggs, M. Ali, H. Gornall, L.R. Couthard, A. Aeby, S.P. Attard-Montalto, E. Bertini, C. Bodemer, K. Brockmann, L.A. Brueton, P.C. Corry, I. Desguerre, E. Fazzi, A.G. Cazorla, B. Gener, B.C. Hamel, A. Heiberg, M. Hunter, M.S. van der Knaap, R. Kumar, L. Lagae, P.G. Landrieu, C.M. Lourenco, D. Marom, M.F. McDermott, W. van der Merwe, S. Orcesi, J.S. Prendiville, M. Rasmussen, S.A. Shalev, D.M. Soler, M. Shinawi, R. Spiegel, T.Y. Tan, A. Vanderver, E.L. Wakeling, E. Wassmer, E. Whittaker, P. Lebon, D.B. Stetson, D.T. Bonthron, Y.J. Crow, Mutations involved in aicardi-goutieres syndrome implicate SAMHD1 as regulator of the innate immune response, Nat. Genet. 41 (2009) 829-832.

[44] A. Brandariz-Nunez, J.C. Valle-Casuso, T.E. White, N. Laguette, M. Benkirane, J. Brojatsch, F. Diaz-Griffero, Role of SAMHD1 nuclear localization in restriction of HIV-1 and SIVmac, Retrovirology. 9 (2012) 49.

[45] F. Qiao, J.U. Bowie, The many faces of SAM, Sci. STKE. 2005 (2005) re7.

[46] L. Aravind, E.V. Koonin, The HD domain defines a new superfamily of metal-dependent phosphohydrolases, Trends Biochem. Sci. 23 (1998) 469-472.

[47] N. Li, W. Zhang, X. Cao, Identification of human homologue of mouse IFN-gamma induced protein from human dendritic cells, Immunol. Lett. 74 (2000) 221-224.

[48] N. Laguette, B. Sobhian, N. Casartelli, M. Ringeard, C. Chable-Bessia, E. Segeral, A. Yatim, S. Emiliani, O. Schwartz, M. Benkirane, SAMHD1 is the dendritic- and myeloid-cell-specific HIV-1 restriction factor counteracted by vpx, Nature. 474 (2011) 654-657.

[49] H. Lahouassa, W. Daddacha, H. Hofmann, D. Ayinde, E.C. Logue, L. Dragin, N. Bloch, C. Maudet, M. Bertrand, T. Gramberg, G. Pancino, S. Priet, B. Canard, N. Laguette, M. Benkirane, C. Transy, N.R. Landau, B. Kim, F. Margottin-Goguet, SAMHD1 restricts the replication of human immunodeficiency virus type 1 by depleting the intracellular pool of deoxynucleoside triphosphates, Nat. Immunol. 13 (2012) 223-228.

[50] S.R. Kornberg, I.R. Lehman, M.J. Bessman, E.S. Simms, A. Kornberg, Enzymatic cleavage of deoxyguanosine triphosphate to deoxyguanosine and tripolyphosphate, J. Biol. Chem. 233 (1958) 159-162.

[51] N. Kondo, S. Kuramitsu, R. Masui, Biochemical characterization of TT1383 from thermus thermophilus identifies a novel dNTP triphosphohydrolase activity stimulated by dATP and dTTP, J. Biochem. 136 (2004) 221-231.

[52] I.I. Vorontsov, G. Minasov, O. Kiryukhina, J.S. Brunzelle, L. Shuvalova, W.F. Anderson, Characterization of the deoxynucleotide triphosphate triphosphohydrolase (dNTPase) activity of the EF1143 protein from enterococcus faecalis and crystal structure of the activator-substrate complex, J. Biol. Chem. 286 (2011) 33158-33166.

[53] D. Kumar, J. Viberg, A.K. Nilsson, A. Chabes, Highly mutagenic and severely imbalanced dNTP pools can escape detection by the S-phase checkpoint, Nucleic Acids Res. 38 (2010) 3975-3983.

[54] M. Meuth, The molecular basis of mutations induced by deoxyribonucleoside triphosphate pool imbalances in mammalian cells, Exp. Cell Res. 181 (1989) 305-316.

[55] D. Kumar, A.L. Abdulovic, J. Viberg, A.K. Nilsson, T.A. Kunkel, A. Chabes, Mechanisms of mutagenesis in vivo due to imbalanced dNTP pools, Nucleic Acids Res. 39 (2011) 1360-1371.

[56] R. Hirschhorn, Adenosine deaminase deficiency, Immunodefic. Rev. 2 (1990) 175-198.

[57] L. Leanza, C. Miazzi, P. Ferraro, P. Reichard, V. Bianchi, Activation of guanine-beta-D-arabinofuranoside and deoxyguanosine to triphosphates by a common pathway blocks T lymphoblasts at different checkpoints, Exp. Cell Res. 316 (2010) 3443-3453.

[58] M.L. Markert, Purine nucleoside phosphorylase deficiency, Immunodefic. Rev. 3 (1991) 45-81.

[59] A. Spinazzola, F. Invernizzi, F. Carrara, E. Lamantea, A. Donati, M. Dirocco, I. Giordano, M. Meznaric-Petrusa, E. Baruffini, I. Ferrero, M. Zeviani, Clinical and molecular features of mitochondrial DNA depletion syndromes, J. Inherit. Metab. Dis. 32 (2009) 143-158.

[60] I. Nishino, A. Spinazzola, M. Hirano, Thymidine phosphorylase gene mutations in MNGIE, a human mitochondrial disorder, Science. 283 (1999) 689-692.

[61] H. Mandel, R. Szargel, V. Labay, O. Elpeleg, A. Saada, A. Shalata, Y. Anbinder, D. Berkowitz, C. Hartman, M. Barak, S. Eriksson, N. Cohen, The deoxyguanosine kinase gene is mutated in individuals with depleted hepatocerebral mitochondrial DNA, Nat. Genet. 29 (2001) 337-341.

[62] A. Saada, A. Shaag, H. Mandel, Y. Nevo, S. Eriksson, O. Elpeleg, Mutant mitochondrial thymidine kinase in mitochondrial DNA depletion myopathy, Nat. Genet. 29 (2001) 342-344.

[63] C. Rampazzo, P. Ferraro, G. Pontarin, S. Fabris, P. Reichard, V. Bianchi, Mitochondrial deoxyribonucleotides, pool sizes, synthesis, and regulation, J. Biol. Chem. 279 (2004) 17019-17026.

[64] C. Gazziola, M. Moras, P. Ferraro, L. Gallinaro, R. Verin, C. Rampazzo, P. Reichard, V. Bianchi, Induction of human high K(M) 5'-nucleotidase in cultured 293 cells, Exp. Cell Res. 253 (1999) 474-482.

[65] M.P. King, G. Attardi, Isolation of human cell lines lacking mitochondrial DNA, Methods Enzymol. 264 (1996) 304-313.

[66] C. Rampazzo, S. Fabris, E. Franzolin, K. Crovatto, M. Frangini, V. Bianchi, Mitochondrial thymidine kinase and the enzymatic network regulating thymidine triphosphate pools in cultured human cells, J. Biol. Chem. 282 (2007) 34758-34769.

[67] M.W. Pfaffl, A new mathematical model for relative quantification in real-time RT-PCR, Nucleic Acids Res. 29 (2001) e45.

[68] P.A. Sherman, J.A. Fyfe, Enzymatic assay for deoxyribonucleoside triphosphates using synthetic oligonucleotides as template primers, Anal. Biochem. 180 (1989) 222-226.

[69] P. Ferraro, E. Franzolin, G. Pontarin, P. Reichard, V. Bianchi, Quantitation of cellular deoxynucleoside triphosphates, Nucleic Acids Res. 38 (2010) e85.

[70] N. Beloglazova, R. Flick, A. Tchigvintsev, G. Brown, A. Popovic, B. Nocek, A.F. Yakunin, Nuclease activity of the human SAMHD1 protein implicated in the aicardi-goutieres syndrome and HIV-1 restriction, J. Biol. Chem. 288 (2013) 8101-8110.

[71] G. Pontarin, A. Fijolek, P. Pizzo, P. Ferraro, C. Rampazzo, T. Pozzan, L. Thelander, P.A. Reichard, V. Bianchi, Ribonucleotide reduction is a cytosolic process in mammalian cells independently of DNA damage, Proc. Natl. Acad. Sci. U. S. A. 105 (2008) 17801-17806.

[72] S.M. Amie, R.A. Bambara, B. Kim, GTP is the primary activator of the anti-HIV restriction factor SAMHD1, J. Biol. Chem. 288 (2013) 25001-25006.

[73] C. Zhu, W. Gao, K. Zhao, X. Qin, Y. Zhang, X. Peng, L. Zhang, Y. Dong, W. Zhang, P. Li, W. Wei, Y. Gong, X.F. Yu, Structural insight into dGTP-dependent activation of tetrameric SAMHD1 deoxynucleoside triphosphate triphosphohydrolase, Nat. Commun. 4 (2013) 2722.

[74] I.I. Vorontsov, Y. Wu, M. Delucia, G. Minasov, J. Mehrens, L. Shuvalova, W.F. Anderson, J. Ahn, Mechanisms of allosteric activation and inhibition of the deoxyribonucleoside triphosphate triphosphohydrolase from enterococcus faecalis, J. Biol. Chem. (2013) .

[75] A. Cribier, B. Descours, A.L. Valadao, N. Laguette, M. Benkirane, Phosphorylation of SAMHD1 by cyclin A2/CDK1 regulates its restriction activity toward HIV-1, Cell. Rep. 3 (2013) 1036-1043.

[76] Y. Engstrom, B. Rozell, H.A. Hansson, S. Stemme, L. Thelander, Localization of ribonucleotide reductase in mammalian cells, EMBO J. 3 (1984) 863-867.

[77] Y. Engstrom, B. Rozell, Immunocytochemical evidence for the cytoplasmic localization and differential expression during the cell cycle of the M1 and M2 subunits of mammalian ribonucleotide reductase, EMBO J. 7 (1988) 1615-1620.

[78] E. Franzolin, G. Pontarin, C. Rampazzo, C. Miazzi, P. Ferraro, E. Palumbo, P. Reichard, V. Bianchi, The deoxynucleotide triphosphohydrolase SAMHD1 is a major regulator of DNA precursor pools in mammalian cells, Proc. Natl. Acad. Sci. U. S. A. 110 (2013) 14272-14277.

[79] M.G. Careddu, S. Allegrini, R. Pesi, M. Camici, M. Garcia-Gil, M.G. Tozzi, Knockdown of cytosolic 5'-nucleotidase II (cN-II) reveals that its activity is essential for survival in astrocytoma cells, Biochim. Biophys. Acta. 1783 (2008) 1529-1535.

[80] G. Pontarin, P. Ferraro, C. Rampazzo, G. Kollberg, E. Holme, P. Reichard, V. Bianchi, Deoxyribonucleotide metabolism in cycling and resting human fibroblasts with a missense mutation in p53R2, a subunit of ribonucleotide reductase, J. Biol. Chem. 286 (2011) 11132-11140.

[81] A. Gupta, S. Sharma, P. Reichenbach, L. Marjavaara, A.K. Nilsson, J. Lingner, A. Chabes, R. Rothstein, M. Chang, Telomere length homeostasis responds to changes in intracellular dNTP pools, Genetics. 193 (2013) 1095-1105.

[82] S. de Silva, H. Hoy, T.S. Hake, H.K. Wong, P. Porcu, L. Wu, Promoter methylation regulates SAMHD1 gene expression in human CD4+ T cells, J. Biol. Chem. 288 (2013) 9284-9292.

[83] T.E. White, A. Brandariz-Nunez, J.C. Valle-Casuso, S. Amie, L.A. Nguyen, B. Kim, M. Tuzova, F. Diaz-Griffero, The retroviral restriction ability of SAMHD1, but not its deoxynucleotide triphosphohydrolase activity, is regulated by phosphorylation, Cell. Host Microbe. 13 (2013) 441-451.

[84] B. Stillman, Deoxynucleoside triphosphate (dNTP) synthesis and destruction regulate the replication of both cell and virus genomes, Proc. Natl. Acad. Sci. U. S. A. 110 (2013) 14120-14121.

[85] A. Chabes, B. Stillman, Constitutively high dNTP concentration inhibits cell cycle progression and the DNA damage checkpoint in yeast saccharomyces cerevisiae, Proc. Natl. Acad. Sci. U. S. A. 104 (2007) 1183-1188.

[86] Y.J. Crow, J. Rehwinkel, Aicardi-goutieres syndrome and related phenotypes: Linking nucleic acid metabolism with autoimmunity, Hum. Mol. Genet. 18 (2009) R130-6.

[87] K. Zhao, J. Du, X. Han, J.L. Goodier, P. Li, X. Zhou, W. Wei, S.L. Evans, L. Li, W. Zhang, L.E. Cheung, G. Wang, H.H. Kazazian Jr, X.F. Yu, Modulation of LINE-1 and Alu/SVA retrotransposition by aicardi-goutieres syndrome-related SAMHD1, Cell. Rep. 4 (2013) 1108-1115.

[88] E. Leshinsky-Silver, G. Malinger, L. Ben-Sira, D. Kidron, S. Cohen, S. Inbar, T. Bezaleli, A. Levine, C. Vinkler, D. Lev, T. Lerman-Sagie, A large homozygous deletion in the SAMHD1 gene causes atypical aicardi-goutieres syndrome associated with mtDNA deletions, Eur. J. Hum. Genet. 19 (2011) 287-292.